

In presenting the dissertation as a partial fulfillment of the requirements for an advanced degree from the Georgia Institute of Technology, I agree that the Library of the Institute shall make it available for inspection and circulation in accordance with its regulations governing materials of this type. I agree that permission to copy from, or to publish from, this dissertation may be granted by the professor under whose direction it was written, or, in his absence, by the Dean of the Graduate Division when such copying or publication is solely for scholarly purposes and does not involve potential financial gain. It is understood that any copying from, or publication of, this dissertation which involves potential financial gain will not be allowed without written permission.

J U

3/17/65

b

RAREFIED GAS FLOW BETWEEN
TWO PARALLEL PLATES
FOR THREE MOLECULAR MODELS

A THESIS

Presented to

The Faculty of the Graduate Division

by

Robert Lee Stoy, Jr.

In Partial Fulfillment
of the Requirements for the Degree
Doctor of Philosophy in the
School of Aerospace Engineering

Georgia Institute of Technology

May, 1966

RAREFIED GAS FLOW BETWEEN
TWO PARALLEL PLATES.
FOR THREE MOLECULAR MODELS

Approved:

Chairman

Date approved by Chairman:

5/20/66

ACKNOWLEDGMENTS

The author expresses his appreciation to Dr. A. Ben Huang, his thesis advisor, for his suggestion of the thesis topic and for his assistance in the development of this study. He also thanks Dr. Arnold L. Ducoffe and Dr. James Wu for serving on the Reading Committee.

Also, the author expresses his gratitude to his fellow graduate students, Mr. Joseph D. Stewart and Mr. Don P. Giddens, for the time they have spent discussing problems associated with this dissertation.

The author is grateful for the NASA Fellowship that has provided for three years of graduate study.

In addition, the author wishes to thank his parents, Mr. and Mrs. Robert L. Stoy, Sr., for their assistance and support during his undergraduate and graduate study.

Finally, the author is especially grateful to his wife, Sally, for the encouragement and patience she has shown during this time. Her assistance in the preparation of the preliminary draft is gratefully acknowledged.

TABLE OF CONTENTS

	Page
ACKNOWLEDGMENTS	ii
LIST OF TABLES	v
LIST OF ILLUSTRATIONS	vi
SUMMARY	vii
NOMENCLATURE	xi
Chapter	
I. INTRODUCTION AND HISTORICAL BACKGROUND	1
Purpose and Scope of Work	
Historical Background	
Review of Recent Literature	
II. METHOD OF SOLUTION	10
Krook Model	
Hard Sphere Model	
Maxwellian Model	
III. DISCUSSION OF RESULTS	40
Experimental Data	
Krook Model	
Hard Sphere Model	
Maxwellian Model	
IV. CONCLUSIONS AND RECOMMENDATIONS	68
APPENDICES	
A. DERIVATION OF EQUATIONS USED IN THE FULL-RANGE METHOD FOR THE KROOK MODEL	71
B. SOLUTION OF THE FIRST APPROXIMATION FOR THE FULL- RANGE MOMENT METHOD USING THE KROOK MODEL	76
C. DERIVATION OF EQUATIONS USED IN THE HALF-RANGE METHOD FOR THE KROOK MODEL	78

TABLE OF CONTENTS (Continued)

APPENDICES	Page
D. SOLUTION OF THE SECOND APPROXIMATION FOR THE HALF-RANGE MOMENT METHOD USING THE KROOK MODEL	82
E. DERIVATION OF THE FREE-MOLECULAR LIMIT FOR THE VOLUME FLOW RATE USING THE WILLIS ITERATION METHOD	85
F. SOLUTION OF THE SECOND APPROXIMATION FOR THE HALF-RANGE MOMENT METHOD USING THE HARD SPHERE MODEL	88
G. THE CALCULATION OF I_8 FOR THE MAXWELLIAN MODEL	92
LITERATURE CITED	96
VITA	99

LIST OF TABLES

Table	Page
1. Volume Flow Rate Versus Inverse Knudsen Number for the Third Approximation by the Full-Range Method for the Krook Model	44
2. Volume Flow Rate Versus Inverse Knudsen Number for the Third Approximation by the Half-Range Method for the Krook Model	46
3. Volume Flow Rate Versus Inverse Knudsen Number for the Second Approximation by the Half-Range Method for the Hard Sphere Model	50
4. Volume Flow Rate Versus Inverse Knudsen Number for the Second Approximation by the Half-Range Method for the Hard Sphere Model	55
5. Volume Flow Rate Versus Inverse Knudsen Number for the Second Approximation by the Half-Range Method for the Maxwellian Model	62
6. Volume Flow Rate Versus Inverse Knudsen Number for the Third Approximation by the Half-Range Method for the Maxwellian Model	63

LIST OF ILLUSTRATIONS

Figure	Page
1. Geometry of the Problem	2
2. Volume Flow Rate Versus Inverse Knudsen Number for the Krook Model, Full-Range Moment Method	45
3. Volume Flow Rate Versus Inverse Knudsen Number for the Krook Model, Half-Range Moment Method	47
4. Volume Flow Rate Versus Inverse Knudsen Number for the Krook Model, Willis Iteration Method	51
5. Volume Flow Rate Versus Inverse Knudsen Number for the Hard Sphere Model, Hydrogen	56
6. Volume Flow Rate Versus Inverse Knudsen Number for the Hard Sphere Model, Helium	57
7. Volume Flow Rate Versus Inverse Knudsen Number for the Hard Sphere Model, Carbon Dioxide	58
8. Volume Flow Rate Versus Inverse Knudsen Number for the Maxwellian Model, Hydrogen	64
9. Volume Flow Rate Versus Inverse Knudsen Number for the Maxwellian Model, Helium	65
10. Volume Flow Rate Versus Inverse Knudsen Number for the Maxwellian Model, Carbon Dioxide	66

SUMMARY

An analytic solution of the Boltzmann equation for the problem of a gas flowing between two parallel, infinite plates, applicable for all flow regimes, has been developed for three different molecular models. The molecular models are the Krook, hard sphere, and Maxwellian models. The full-range and half-range moment methods, with the Willis iteration method, were used in the analysis. The purpose of this dissertation was to make a meaningful comparison of the volume flow rate with the existing experimental data, and to adequately describe the minimum in the volume flow rate which occurs in the transition regime.

The physical problem is that of a gas flowing through a long, wide channel at low speed. The mathematical problem has been idealized to consider a one-component gas flowing between two parallel, infinite plates. As a result of this idealization the mass velocity profiles are considered fully developed. Although the theoretical analysis ignores the end effects present in a finite channel, the quantity of interest is the volume flow rate which remains the same regardless which section of the channel is considered. Thus, the mathematical problem suitably describes the conditions -- as far as the volume flow rate is concerned -- existing near the mid-point of a long channel.

The theoretical analysis was based on the following assumptions:

1. There was no density variation between the plates at any given longitudinal station.
2. The flow field and plates were at the same temperature and

were isothermal.

3. In position-space, the mass velocity varied only in the direction normal to the plates.

4. The pressure gradient was constant.

The Boltzmann equation with the Krook model was first solved using the full-range moment method. In this method, the perturbation of the distribution function is expanded in a polynomial in c_x , the normal velocity component. The coefficients are functions of position and are determined by the solution of the moment equations obtained from the Boltzmann equation. The moments are defined over the full velocity range, from $-\infty$ to $+\infty$. The first three approximations for the full-range method were obtained. Since the convergence was slow and no minimum was obtained in the transition regime, the solution was not carried further by this method.

After applying the full-range method and not achieving satisfactory results, the half-range moment method was applied to the Boltzmann equation using the Krook model. The method is similar to the full-range method, except that the perturbation of the distribution function is explicitly divided into two streams. In addition, the moments are defined over the half ranges, $-\infty$ to $+\infty$. The first three approximations by the half-range method were obtained. The third approximation yielded the desired minimum in the transition regime. For the transition, slip, and continuum regimes there was very good agreement with the experimental data. However, in the near-free-molecular regime the theoretical analysis yielded poor results. Thus, the Willis iteration method was applied to improve the results in this region.

This method consists of developing, from the basic integrodifferential equation, a relation for the volume flow rate in terms of a first guess of the volume flow rate. Once a first guess is known, the first iteration can be computed. As a first guess, the first approximation for the Krook model was used. The result of the first iteration showed the correct limit for free-molecular flow, indicating good agreement with the experimental data.

The Boltzmann equation with the hard sphere model was solved by the half-range method for two approximations. The second approximation yielded a minimum in the volume flow rate in the transition regime. Data for helium, hydrogen, and carbon dioxide were compared to the theoretical results and good agreement was obtained in all but the near-free-molecular region.

The last analysis was that of the Maxwellian model using the half-range method. The first three approximations were solved, and the third yielded the desired minimum in the volume flow rate in the transition region. Data for helium, hydrogen, and carbon dioxide were compared with the theory and good agreement was obtained for all but the near-free-molecular region. It was necessary to calculate values of five bracket integrals, which have not been previously calculated, for the third approximation.

The consistently unsatisfactory agreement in the near-free-molecular region for all the molecular models is a result of the polynomial approximation method. The volume flow rate exhibits a non-analytic behavior for near-free-molecular conditions, and it is impossible to obtain this behavior from a finite number of terms in a polynomial.

It was concluded that the half-range method yielded good results for the transition, slip, and continuum regions. By using the Willis iteration, this good agreement with the experimental data was extended to all of the flow regimes. The Krook model was a satisfactory approximation to the collision integral of the Boltzmann equation, yielding better results than the hard sphere or Maxwellian models.

NOMENCLATURE

Symbol

\AA	Angstrom unit, 10^{-8} cm.
A_i^{\pm}	see equation (9)
a	molecular diameter
B_i^{\pm}	see equation (28)
\bar{c}	nondimensional velocity, $\beta \bar{v}$
c_1	βv_1
d	plate separation distance
f	distribution function
f_0	local Maxwellian distribution function
f_{eq}	equilibrium distribution function
$f_m(x)$	see equation (56)
H_i	Hermite polynomials
h	perturbation of distribution function
h^*	nondimensional perturbation, $h/\kappa d$
I_i	bracket integral, see equation (67)
$J(\)$	collision integral, see equation (61)
k	Boltzmann constant
L_i^{\pm}	orthogonal polynomial, see equation (C.3)
M	molecular weight
M_k	full-range moments, see equation (10)
m	molecular mass

Symbol

n	number density
n_0	local number density
p	pressure
p_i	inlet pressure
p_0	local pressure
Q	volume flow rate
q	nondimensional mass velocity
$q_{z_{avg}}$	average velocity at any cross-section
R_1	force constant for Maxwellian molecules
T	temperature
t	time
u	mass velocity
V	volume
\bar{v}	molecular velocity
v_1	velocity of one molecule in a binary collision
v_c	velocity of center of mass in a binary collision
v_r	relative velocity between molecules in a binary collision
x, y, z	position coordinates

Greek Symbols

α	constant, see equation (D.9)
β	$m/2kT$
δ	inverse Knudsen number, Krook model
δ_m	inverse Knudsen number, Maxwellian model
δ_s	inverse Knudsen number, hard sphere model

Greek Symbols

δ_{ij}	Kronecker delta function
ε	angle, see equation (58)
η	nondimensional coordinate, x/d
η	viscosity
θ	scattering angle, see equation (58)
κ	$(dp/dz)/p_i$
λ	mean free path, Krook model, $\sigma_1/\beta n_0$
π	constant = 3.14159265359
σ	tangential accommodation coefficient
σ_1	$n/\sigma_1 =$ collision frequency
ψ	h^*/c_z

Superscripts

\pm indicates positive and negative direction of c_x

Subscripts

x, y, z direction components

CHAPTER I

INTRODUCTION AND HISTORICAL BACKGROUND

Purpose and Scope of WorkDiscussion of the Problem

The solution of the parallel-plate geometry flow problem is of interest, first, because deviations from the continuum theory have been found in the experimental data for low pressures, and, second, because the simple geometry of the problem provides a further test for the powerful methods of solution recently developed and applied to similar problems.

The problem consists of determining the volume flow rate of a rarefied gas between two parallel, infinite plates. The geometry of the problem is shown in Figure 1, page 2. The physical problem is that of a gas flowing through a long, wide channel (such that the height-to-width ratio is very small) at low speed. The mathematical problem has been idealized to consider a one-component gas flowing between two parallel, infinite plates. As a result of this idealization the velocity profiles are "fully" developed (that is, there is no change in the macroscopic velocity in the longitudinal direction). Although the mathematical problem ignores the end effects present in a finite channel, the quantity of interest is the volume flow rate which remains the same regardless which section of the finite channel is considered. Thus, the idealized mathematical problem suitably describes the conditions -- as far as the volume flow rate is concerned -- existing near the mid-point of a long channel.

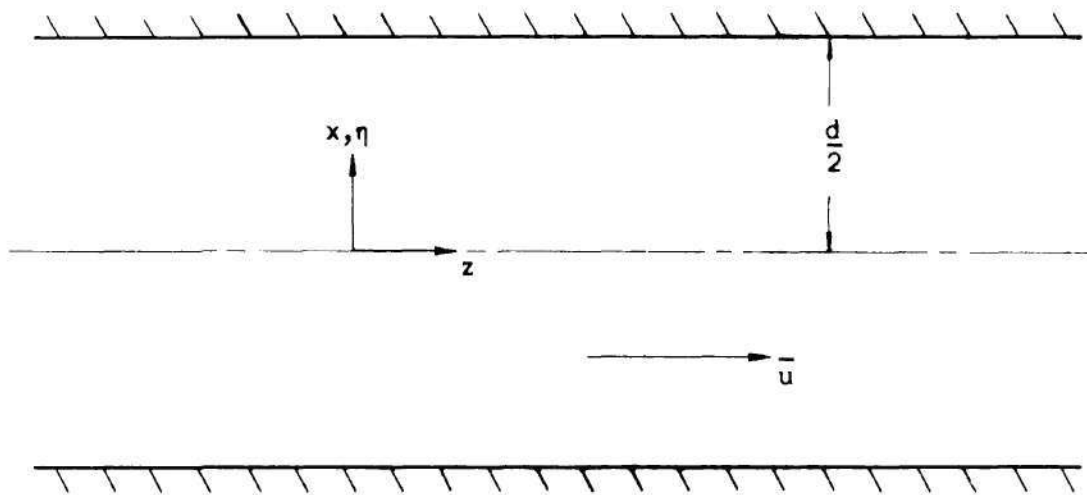


Figure 1. Geometry of the Problem.

Purpose

The purpose of the present work is:

1. To solve the Boltzmann equation, analytically, for the distribution function of a gas flowing between two infinite, parallel plates for three different molecular models, i.e., the Krook, hard sphere, and Maxwellian models.

2. To make a meaningful comparison of the volume flow rate with the existing experimental data for several different gases.

3. To demonstrate that it is possible to obtain a satisfactory solution of the volume flow rate for the free-molecular, transition, slip, and continuum flow regimes.

Scope of the Investigation

The Boltzmann equation using the Krook model is first solved by the full-range moment method (described in Gross, Jackson, and Ziering, (1)), and then by the half-range moment method (1). The solution by the half-range moment method is then iterated once following the method of Willis (2). The results of these solutions are then compared with Cercignani's (3) numerical results and Dong's (4) experimental data for the volume flow rate. Next, the Boltzmann equation using the hard sphere model is solved by the half-range method, and the results are compared with the experiments of Dong. Last, the Boltzmann equation using the Maxwellian model is solved by the half-range method, and the results are compared with the experiments of Dong.

Historical Background

The earliest work on parallel plates and the related problem of

rarefied gas flow in tubes was that of Knudsen. He developed, in 1909, an equation for the volume flow rate in long, circular tubes for free-molecular flow (5). In the same paper he presented an equation for the volume flow rate in finite length, rectangular channels under the condition of free-molecular flow. Both of these equations were derived from a consideration of the momentum flux and the pressure forces. Knudsen also presented some results of his experiments with long tubes in this paper, and demonstrated that a minimum in the volume flow rate exists in the transition regime. He showed that this minimum could be observed only by reducing the pressure in the system to one mm. of mercury or less. Further work on Knudsen's part substantiated the existence of the minimum (6). Knudsen described his early work in a short monograph (7), which, unlike his previous works, was written in English.

Knudsen's derivations of the flow rate equations were somewhat inaccurate because of some non-rigorous assumptions on his part. Von Smoluchowski (8) rigorously derived an expression for the volume flow rate in a long cylinder for free-molecular flow. Besides extending Knudsen's work to any cross section, he introduced the possibility of non-diffuse reflection of the molecules from the tube walls.

Further experimental work with parallel-plate geometry was carried out by Gaede (9) in 1913. His work further verified the existence of a minimum in the volume flow rate. Gaede used two parallel plates, 4×10^{-4} cm. apart; the width of the slit was 3.4 cm.; the dimension in the direction of flow was 0.12 cm. Thus, he worked with essentially a two-dimensional slit. Gaede observed that the volume flow rate at the minimum was about fifty percent below the theoretical free-molecular value.

Clausing (10), in his work of 1932, derived an expression for the volume flow rate between parallel plates in free-molecular conditions. He considered the slit to be infinitely wide; consequently, only the length of the plates and the distance between the plates were parameters in his equation. His equation is applicable for both long and short plates.

In 1937, Rasmussen (11) carried out experiments to determine the volume flow rate for parallel-plate geometry for low pressures. In these experiments, Rasmussen used two glass plates, 1.82×10^{-3} cm. apart. The width of the slit was 1.32 cm. and the dimension in the direction of flow was 0.963 cm. He observed a minimum in the volume flow rate near a Knudsen number of unity.

These early experiments established that a minimum existed in the volume flow rate at very low pressures. This minimum was not predicted by the continuum-flow theory, and, furthermore, no theory was available to predict the minimum.

Certainly, a need existed for a theory to adequately predict the properties of the gas flow between parallel plates (and tubes) for the entire Knudsen number range. A review of the attempts to adequately determine the volume flow rate for the parallel plate geometry is presented in the next section.

Review of Recent Literature

After the work of the early investigators, it was not until 1952 that a theoretical analysis was presented to determine the volume flow rate between parallel plates. Hiby and Pahl (12), following the work that Pollard and Present (13) had presented on circular tubes, derived an

expression for the volume flow rate in a rectangular channel of infinite length for near-free-molecular flow. Unfortunately, they considered only the self-diffusion component of the flow rate, and did not include the component resulting from the presence of a pressure drop. Consequently, their results did not agree with the available experimental data and did not indicate the existence of a minimum.

The analysis of Hiby and Pahl was corrected by Dong (4) in 1956. He accounted for the flow due to the pressure gradient. As a result of the correction, Hiby and Pahl's theoretical work presented a minimum in the transition region, and agreed with Dong's experimental work. However, this solution is inaccurate for Knudsen numbers less than unity, so that the continuum-flow solution is not predictable. Dong determined the volume flow rate for a gas moving between two parallel plates 0.324 cm. apart, 22.86 cm. wide, and 61.0 cm. long. The experiments were run with H_2 , He, air, CO_2 , and freon-12.

Neither Hiby and Pahl nor Dong were able to calculate any quantity other than the volume flow rate, since their analyses were not carried out by solving the Boltzmann equation and determining the distribution function. Their solutions were found by considering the flux of particles leaving the walls of the channel and the flux of particles leaving points of collision in the gas. Both investigators assumed that only one molecule-molecule collision occurred between collisions with the wall.

Thus, there are two drawbacks to the work of these investigators: One, only the volume flow rate was determined; two, the analyses were not applicable throughout the entire Knudsen number range.

Takao (14), in 1960, was able to solve the Boltzmann equation (using the Krook model for the collision term) and to obtain a minimum in

his solution of the volume flow rate for the parallel-plate geometry problem. His solution is applicable for the entire Knudsen number range from continuum to free-molecular flow. Takao's method consisted of dividing the distribution function at any point in the channel into two parts; those molecules passing the point which have not suffered a collision since their reflection from the wall, and those molecules which have collided with other molecules since their reflection. Since this approach is quite involved, Takao found it necessary to make physical and mathematical assumptions which were not rigorously supported. Also, Takao found that it was not possible to distinguish between gases. Consequently, the validity of his results (as far as quantitative results are concerned) is questionable and the results are limited.

Ziering (15), in 1960, solved this same problem for the distribution function and, subsequently, obtained the volume flow rate. However, his solution did not exhibit the desired minimum because he omitted a term in the Boltzmann equation.

Cercignani (3), (16), in 1962, pointed out corrections to Takao's work, and numerically solved the Boltzmann equation (with the Krook model) for the volume flow rate throughout the entire Knudsen number range. He first assumed the distribution function to be perturbed slightly from its equilibrium value. After developing the Boltzmann equation in terms of the perturbation, he carried out certain integrations to obtain an integral equation for the velocity and then integrated the velocity between the two plates to obtain the volume flow rate. Cercignani used a numerical method to solve the integral equation for the velocity and, subsequently, the volume flow rate. Although his results were in reasonable agreement

with the experimental data, the numerical procedure was complicated and only the volume flow rate for the Krook model was determined. Because of the use of the Krook model, there was no distinction between gases. Cercignani's solution was based on the assumptions of completely diffuse reflection of the molecules from the plates and of a constant pressure gradient.

The method used in the present work to solve the Boltzmann equation is the half-range moment method. A good description of this method is given in Gross, Jackson, and Ziering (1), where the method was used to solve the Boltzmann equation for the Couette flow problem. Briefly, the half-range moment method assumes that the flow is divided into two streams, one stream leaving the wall, and one stream approaching the wall. The perturbation of the distribution function is then expanded in a series of orthogonal polynomials which are orthogonal over the velocity half-ranges, $-\infty < \bar{v} < 0$ and $0 < \bar{v} < \infty$. It is then possible to determine the solution of the Boltzmann equation for the perturbation of the distribution function.

This concept of dividing the flow into two streams, with orthogonality conditions imposed over the half-range, is accredited to Yvon, as discussed by Kourganoff and Busbridge (17) on page 101 of their work. The method arose from an investigation on neutron diffusion, and was subsequently used by Gross and Ziering (18) in 1956, in the Milne problem for a plane gray atmosphere with isotropic radiation. These problems, and that of flow between parallel plates, have as a basic equation a similar integrodifferential equation. Furthermore, an interaction occurs at the boundary of each problem such that the incoming stream is altered

upon reflection from the boundary. Thus, there is a discontinuity at the boundary which only the half-range method suitably describes. The similarities between the gasdynamic Boltzmann equation and the radiative Milne equation and their respective boundary conditions are discussed by Huang and Giddens (35).

The half-range method has been successfully applied by Gross, Jackson, and Ziering to the Couette flow problem in a series of reports (1), (19), (20), (21). These reports deal with the Couette problem using the Krook model, hard sphere model, and Maxwellian model in the collision integral of the Boltzmann equation. They solve both the momentum and heat transfer problems with satisfactory results.

The intent of this study is to extend the previous work by analytically solving the Boltzmann equation, using the full-range and half-range moment methods, for three different molecular models. The results for the volume flow rate are compared to the experimental data of Rasmussen and Dong.

CHAPTER II

METHOD OF SOLUTION

Krook ModelGeneral

The problem consists of a fully developed flow between two parallel, infinite plates as shown in Figure 1. The plate separation distance is d and the flow is in the z -direction.

As in all rarefied gas dynamic problems, the Boltzmann equation is the basic transport equation. In the absence of external forces and time variation of properties, the Boltzmann equation is

$$\bar{v} \cdot \frac{\partial f}{\partial \bar{x}} = \left(\frac{df}{dt} \right)_c \quad (1)$$

where the right-hand side of the equation expresses the total variation of f due to molecular collisions. One of the simplest expressions thus far devised for the collision term is the Bhatnager, Gross, and Krook linearized model (22),

$$\left(\frac{df}{dt} \right)_c = \frac{n}{\sigma_1} (f_{eq} - f), \quad (2)$$

where f_{eq} is the local Maxwellian equilibrium distribution function. The linearization of f_{eq} follows that of reference (1) and will not be repeated here.

The mathematical analysis in this study is based upon the

following assumptions:

1. There is no density variation between the plates at any given longitudinal station.
2. The flow field and plates are at the same temperature and are isothermal.
3. In position-space, the mass velocity is a function only of x .
4. The pressure gradient is constant.

In the succeeding sections, the solution for the distribution function by means of the full-range moment method and the half-range moment method is considered. The distribution function for the Krook model is first determined by the full-range moment method, and then by the half-range moment method.

Full-range Moment Method

Basic Equations. Appendix A presents a detailed derivation of the equations involved in the solution by the full-range method. Only the major equations are presented and discussed in this section. The derivation of the equations closely follows that of reference (1) where the full-range method was used to solve the Couette problem.

The distribution function is assumed to be perturbed slightly from the Maxwellian distribution such that

$$f = f_0 (1 + h) \quad (3)$$

where

$$f_0 = n_0 \beta^3 e^{-\beta^2 \bar{v}^2} / \pi^{3/2} \quad (4)$$

and

$$n_0 = p_0/kT = p_1(1 + \kappa z)/kT \quad (5)$$

The constant " κ " (Appendix A, equation A.5) is proportional to the pressure gradient. Using the previous equations and assumptions and introducing dimensionless variables, the Boltzmann equation becomes

$$c_x \frac{dh^*}{d\eta} + c_z + \delta h^* = 2\delta c_z q_z, \quad (6)$$

where $\delta = d/\lambda$ is the inverse Knudsen number, $\lambda = \sigma_1/\beta n_0$ is the mean free path, and

$$q_z(\eta) = \pi^{-3/2} \int_{-\infty}^{\infty} c_z h^* e^{-\bar{c}^2} d^3 c. \quad (7)$$

Substituting $h^*(\eta) = c_z \psi(\eta)$ into equation (6) and integrating over c_y and c_z yields

$$c_x \frac{d\psi}{d\eta} + 1 + \delta\psi = \frac{\delta}{\sqrt{\pi}} \int_{-\infty}^{\infty} \psi e^{-c_x^2} dc_x. \quad (8)$$

In order to obtain solutions for the velocity profiles, $q_z(\eta)$, and the volume flow rate, it is necessary to solve equation (8) for $\psi(\eta)$. The first step is to assume the solution is of the form

$$\psi^\pm(\eta, c_x) = \sum_{n=0}^{\infty} c_x^n A_n^\pm(\eta), \quad (9)$$

where

$$\psi(\eta) = \psi^+(\eta) \quad \text{for } c_x > 0$$

$$\psi(\eta) = \psi^-(\eta) \quad \text{for } c_x < 0.$$

The full-range moments are defined

$$M_k = \frac{1}{\sqrt{\pi}} \int_{-\infty}^{\infty} c_x^k \psi^{\pm} e^{-c_x^2} dc_x. \quad (10)$$

Multiplying equation (8) by $c_x^k e^{-c_x^2} / \sqrt{\pi}$ and integrating c_x over the full velocity range yields the following set of moment equations

$$\frac{dM_1}{d\eta} = 1 \quad (11)$$

$$\frac{dM_2}{d\eta} = -\delta M_1 \quad (12)$$

$$\frac{dM_3}{d\eta} = -\frac{1}{2} - \delta M_2 + \frac{\delta}{2} M_0 \quad (13)$$

$$\frac{dM_4}{d\eta} = -\delta M_3, \quad \text{etc.} \quad (14)$$

Combining equations (9) and (10) yields

$$M_k = \sum_{n=0}^{\infty} \left[A_n^-(\eta) \int_{-\infty}^0 c_x^{n+k} \frac{e^{-c_x^2}}{\sqrt{\pi}} dc_x + A_n^+(\eta) \int_0^{\infty} c_x^{n+k} \frac{e^{-c_x^2}}{\sqrt{\pi}} dc_x \right]. \quad (15)$$

It is now possible to solve equations (11) - (14) for the M_k in terms

of η . It is also possible to write the M_i in terms of the A_i^\pm using equation (10). From these sets of equations, the A_i^\pm are determined as functions of η .

In order to determine the arbitrary constants arising from the solution of equations (11) - (14), the number of boundary conditions necessary must equal the number of M_i . The boundary condition requires that the distribution function at the plates be composed of two parts: One part is the fraction of molecules reflected diffusely and the other is the fraction reflected specularly. The fraction of molecules reflected diffusely is denoted by σ . Thus,

$$f^\pm(x = \mp \frac{d}{2}, c_x) = \sigma f_0 \left(\frac{1 \pm \text{sign } c_x}{2} \right) + (1 - \sigma) f^\mp(x = \mp \frac{d}{2}, -c_x) \quad (16)$$

In terms of ψ this is

$$\psi^\pm(\eta = \mp \frac{1}{2}, c_x) = (1 - \sigma) \psi^\mp(\eta = \mp \frac{1}{2}, -c_x) \quad (17)$$

If $\sigma = 1$, equation (17) becomes

$$A_i^r \left(\mp \frac{1}{2} \right) = 0 \quad (18)$$

To be consistent with the assumption of a constant pressure gradient, only the case $\sigma = 1.0$ should be considered. However, considering the approximations already made, the results should be nearly correct for σ very near unity.

With the solution of the A_i^\pm complete, $\psi^\pm(\eta)$ can be determined.

Then, $q_z(\eta)$ can be found and, subsequently, $Q(\delta)$, the volume flow rate. The derivation of $Q(\delta)$ appears in Appendix A. The first three approximations for the full-range method of the Krook model are discussed in the next three sections.

First Approximation. For the first approximation assume $\psi^\pm(\eta) = A_0^\pm(\eta)$ and use the first two moment equations. The first approximation is solved in detail in Appendix B and only the solution is presented in this section. The solution for the velocity is

$$q_z(\eta) = \frac{\delta}{2} \eta^2 + \frac{\sqrt{\pi}}{4} \left(\frac{2-\sigma}{\sigma} \right) - \frac{\delta}{8} \quad (19)$$

and the volume flow rate is

$$Q(\delta) = \frac{\delta}{6} + \frac{\sqrt{\pi}}{2} \left(\frac{2-\sigma}{\sigma} \right) . \quad (20)$$

Second Approximation. The perturbation of the distribution function is assumed to be proportional to

$$\psi^\pm(\eta) = A_0^\pm(\eta) + A_1^\pm(\eta) c_x . \quad (21)$$

The method of solution for $q_z(\eta)$ follows that described for the first approximation. In this case, four moment equations are used to solve for A_0^\pm and A_1^\pm . For the case $\sigma = 1$, the velocity between the plates is given by

$$q_z(\eta) = \frac{\delta}{2} \eta^2 + 2 \cosh \delta \eta \left[\frac{1 + \frac{2\sqrt{\pi}}{\delta}}{8 \sinh \frac{\delta}{2} + 4\sqrt{\pi} \cosh \frac{\delta}{2}} \right] + \frac{1}{\delta} - \frac{\delta}{8} + \left[-\frac{1}{2} - \frac{\sqrt{\pi}}{\delta} \right] \left[\frac{2 \cosh \frac{\delta}{2} + \sqrt{\pi} \sinh \frac{\delta}{2}}{2 \sinh \frac{\delta}{2} + \sqrt{\pi} \cosh \frac{\delta}{2}} \right] . \quad (22)$$

The flow rate is

$$Q(\delta) = \frac{\delta}{6} - \frac{2}{\delta} + \left[1 + \frac{2\sqrt{\pi}}{\delta} \right] \left[\frac{2 \cosh \frac{\delta}{2} + \sqrt{\pi} \sinh \frac{\delta}{2}}{2 \sinh \frac{\delta}{2} + \sqrt{\pi} \cosh \frac{\delta}{2}} \right] \\ + \frac{1}{\delta} \left[2 + \frac{4\sqrt{\pi}}{\delta} \right] \left[\frac{\sinh \frac{\delta}{2}}{2 \sinh \frac{\delta}{2} + \sqrt{\pi} \cosh \frac{\delta}{2}} \right]. \quad (23)$$

Third Approximation. In this case,

$$\psi^\pm(\eta) = A_0^\pm(\eta) + A_1^\pm(\eta) c_x + A_2^\pm(\eta) c_x^2. \quad (24)$$

The first six moment equations are used to solve for the A_1^\pm . The fifth and sixth moment equations are, respectively,

$$\frac{dM_5}{d\eta} = -\frac{3}{4} - \delta M_4 + \frac{3}{4} \delta M_0 \quad (25)$$

$$\frac{dM_6}{d\eta} = -\delta M_5. \quad (26)$$

Since the third approximation does not yield a satisfactory solution, and since the expressions for $q_z(\eta)$ and $Q(\delta)$ are very complicated, only tabulated values of $Q(\delta)$ versus δ are presented. These data are given in Table 1, page 44.*

Half-range Moment Method

Basic Equations. Beginning with equation (6), it is possible to formulate a method of solution which exhibits convergence faster than the

* All numerical calculations for this study were carried out on a Burroughs B5500 computer.

full-range method for all velocity moments investigated. Rather than multiply equation (6) by $c_x^k e^{-c_x^2}/\sqrt{\pi}$ and integrate over the full velocity range to obtain the moment equations, the equation is multiplied by a similar term and integrated over the half-ranges $-\infty \leq c_x \leq 0$ and $0 \leq c_x \leq \infty$. The result of this operation is a set of differential equations in the variable $h^{*\pm}$, which is the perturbation of the distribution function for the half-range method. The "+" sign indicates $c_x > 0$; the "-" sign, $c_x < 0$.

Appendix C contains a complete derivation of the basic equations used in the half-range solution, so only a few of the equations are presented in this section. The basic integrodifferential equation is

$$c_x \frac{dh^{*\pm}}{d\eta} + c_z + \delta h^{*\pm} = \frac{2}{\pi^{3/2}} \delta c_z \int c_z h^{*\pm} e^{-c^2} d^3c. \quad (27)$$

Following reference (1), it is assumed that $h^{*\pm}$ can be expanded in terms of Hermite polynomials such that

$$h^{*\pm} = \sum_{ijk} B_{ijk}^{\pm}(\eta) L_i^{\pm}(c_x) H_j(c_y) H_k(c_z). \quad (28)$$

H_j and H_k are the usual Hermite polynomials, and $L_i^{\pm}(c_x)$ is an orthogonal polynomial of c_x whose coefficients are determined by the Gram-Schmidt process.

By multiplying each term of equation (27) by $L_l^{\pm}(c_x) H_m(c_y) H_n(c_z) e^{-c^2}$ and integrating over the half-ranges, the following differential recurrence relation is determined:

$$\frac{d}{d\eta} \left[B_{i-1}^{\pm} \frac{\alpha_{i-1}}{\alpha_i} \pm B_i^{\pm} \left(\frac{\beta_{i+1}}{\alpha_{i+1}} - \frac{\beta_i}{\alpha_i} \right) + B_{i+1}^{\pm} \frac{\alpha_i}{\alpha_{i+1}} \right] + \delta B_i^{\pm} = \left[\frac{\delta}{2} (B_0^+ + B_0^-) - \frac{1}{2\sqrt{2}} \right] \delta_{i0}. \quad (29)$$

The α_i and β_i are the known coefficients of the polynomial $L_i^{\pm}(c_x)$. In terms of the unknown function B_i^{\pm} , the boundary conditions are

$$B_i^{\pm} \left(\mp \frac{1}{2} \right) = (1 - \sigma)(-1)^i B_i^{\mp} \left(\mp \frac{1}{2} \right). \quad (30)$$

Furthermore, the symmetry of the physical problem indicates that

$$B_i^{\pm}(\eta) = (-1)^i B_i^{\mp}(-\eta). \quad (31)$$

The flow velocity is given by

$$q_z(\eta) = \frac{1}{\sqrt{2}} (B_0^+ + B_0^-) \quad (32)$$

and the volume flow rate as

$$Q(\delta) = -2 \int_{-\frac{1}{2}}^{\frac{1}{2}} q_z(\eta) d\eta. \quad (33)$$

It is not possible to solve equation (29) by the method used by Gross, Jackson, and Ziering (1) due to the presence of the term $1/2\sqrt{2}$ in the right-hand side. This term does not appear in their equations since the driving force for the Couette flow is the movement of the walls, not a pressure drop. It is possible to solve equation (29) for any approxi-

mation (i.e., for the i^{th} approximation, all $B_k^{\pm} = 0$, $k \geq i$) by assuming a particular solution of the non-homogeneous equation, which is a polynomial, and then solving the homogeneous equation in a manner similar to that of Gross, Jackson, and Ziering (1).

The first, second, and third approximations for the Krook model are presented in the next three sections. The solution for the first approximation is relatively simple and is presented in full. The second approximation is presented in detail in Appendix D. The solution for the third approximation, due to its length, is presented in a brief form. The iteration method of Willis (2) is presented in the fourth section.

First Approximation. In this approximation, $i = 0$, and

$$h^{*\pm} = B_0^{\pm}(\eta) L_0^{\pm}(c_x) c_z \quad (34)$$

where $L_0^{\pm}(c_x) = \sqrt{2}$. Thus, equation (29) becomes

$$\frac{1}{\sqrt{\pi}} \frac{d}{d\eta} B_0^+ + \frac{\delta}{2} B_0^+ = \frac{\delta}{2} B_0^- - \frac{1}{2\sqrt{2}} \quad (35)$$

$$-\frac{1}{\sqrt{\pi}} \frac{d}{d\eta} B_0^- + \frac{\delta}{2} B_0^- = \frac{\delta}{2} B_0^+ - \frac{1}{2\sqrt{2}} \quad (36)$$

Differentiating (35) yields

$$\frac{d^2 B_0^+}{d\eta^2} = \delta \frac{\pi}{2\sqrt{2}} \quad (37)$$

Solving, and using the symmetry condition yields

$$B_0^+(\eta) = \delta \frac{\pi}{4\sqrt{2}} \eta^2 + a_1 \eta + a_2 \quad (38)$$

$$B_0^-(\eta) = \delta \frac{\pi}{4\sqrt{2}} \eta^2 - a_1 \eta + a_2. \quad (39)$$

The expression for a_1 is obtained by substituting equations (38) and (39) into (35). The result is

$$a_1 = -\sqrt{\pi/8}.$$

The expression for a_2 is found by applying the boundary condition,

$$B_0^+(-\frac{1}{2}) = (1 - \sigma) B_0^-(-\frac{1}{2}). \quad (40)$$

Thus,

$$a_2 = -\frac{\pi}{16\sqrt{2}} \delta - \frac{\sqrt{\pi}}{4\sqrt{2}} \left(\frac{2-\sigma}{\sigma}\right). \quad (41)$$

Hence

$$B_0^\pm(\eta) = \frac{\pi}{4\sqrt{2}} \delta \eta^2 \mp \frac{1}{2} \sqrt{\frac{\pi}{2}} \eta - \frac{\pi}{16\sqrt{2}} \delta - \frac{\sqrt{\pi}}{4\sqrt{2}} \left(\frac{2-\sigma}{\sigma}\right), \quad (42)$$

and

$$q_2(\eta) = \frac{\pi}{4} \delta \eta^2 - \frac{\pi}{16} \delta - \frac{\sqrt{\pi}}{4} \left(\frac{2-\sigma}{\sigma}\right). \quad (43)$$

The volume flow rate is

$$Q(\delta) = \frac{\pi}{12} \delta + \frac{\sqrt{\pi}}{2} \left(\frac{2-\sigma}{\sigma}\right). \quad (44)$$

Second Approximation. For this approximation, all $B_i^\pm = 0$, $i \geq 2$.

Equation (29) yields

$$\frac{dB_0^+}{d\eta} \pm \sqrt{\frac{\pi-2}{2}} \frac{dB_1^+}{d\eta} \pm \frac{\sqrt{\pi}}{2} \delta (B_0^+ - B_0^-) = \mp \frac{1}{2} \sqrt{\frac{\pi}{2}} \quad (45)$$

$$\frac{dB_0^+}{d\eta} \pm \frac{2\sqrt{2}}{(\pi-2)^{3/2}} \frac{dB_1^+}{d\eta} + \sqrt{\frac{2\pi}{\pi-2}} \delta B_1^+ = 0. \quad (46)$$

These four equations, with the boundary conditions for B_0^+ and B_1^+ , are used to solve for the four unknowns, B_0^+ , B_0^- , B_1^+ , and B_1^- . The details are presented in Appendix D. For diffuse reflection, the volume flow rate is

$$Q(\delta) = 0.5642 + 0.1667\delta + g_0^+ \left[2.8284 e^{-\alpha \frac{\delta}{2}} + 7.5593 e^{\alpha \frac{\delta}{2}} - \frac{5.5232}{\delta} (e^{\alpha \frac{\delta}{2}} - e^{-\alpha \frac{\delta}{2}}) \right], \quad (47)$$

where $\alpha = 1.8808$ and

$$g_0^+ = \frac{0.1507 + 0.4680/\delta}{0.2804 e^{-\alpha \frac{\delta}{2}} + 2.4943 e^{\alpha \frac{\delta}{2}}}.$$

Third Approximation. In this case, B_0^+ , B_1^+ , and B_2^+ are the only non-zero terms in the expansion of h^{*+} . The expression for h^{*+} is equivalent to a second-degree polynomial in c_x in which all terms are multiplied by c_z , i.e.,

$$h^{*+} = [c_1(\tau) + c_2(\tau) c_x + c_3(\tau) c_x^2] c_z.$$

The six equations used to solve for the six unknowns are

$$\frac{dB_0^\pm}{d\eta} \pm \sqrt{\frac{\pi-2}{2}} \frac{dB_1^\pm}{d\eta} + \frac{\sqrt{\pi}}{2} \delta(B_0^+ - B_0^-) = -\frac{1}{2} \sqrt{\frac{\pi}{2}} \quad (48)$$

$$\begin{aligned} \frac{dB_0^\pm}{d\eta} \pm \left(\frac{2}{\pi-2}\right)^{3/2} \frac{dB_1^\pm}{d\eta} + \frac{\pi\sqrt{2}\sqrt{\pi-3}}{(\pi-2)^{3/2}} \frac{dB_2^\pm}{d\eta} \\ + \sqrt{\frac{2\pi}{\pi-2}} \delta B_1^\pm = 0 \end{aligned} \quad (49)$$

$$\frac{dB_1^\pm}{d\eta} \pm \frac{(\pi-4)^2}{2\pi(\pi-3)^{3/2}} \frac{dB_2^\pm}{d\eta} + \frac{\pi-2}{\sqrt{\pi}\sqrt{\pi-3}} \delta B_2^\pm = 0. \quad (50)$$

After determining the particular solutions for the B_1^\pm , the non-homogeneous terms in the equations are dropped and the solution is determined in a manner similar to that of the second approximation presented in Appendix D. Following the notation used in the solution of the second approximation, it was found that

$$\begin{aligned} \alpha_1 &= 3.7853 & \alpha_2 &= 0.6421 \\ \ell_1 &= 3.9389 & \ell_2 &= 1.6284 \\ m_1 &= -0.4129 & m_2 &= -0.1757 \\ n_1 &= 4.3029 & n_2 &= 1.0074 \\ p_1 &= 0.1556 & p_2 &= 0.0361 \\ q_1 &= 2.4603 & q_2 &= -2.1690. \end{aligned}$$

The solution for the velocity distribution between the plates is

$$q_z(\eta) = \sqrt{2} b_0 + \frac{1}{2} \eta^2 + 4.9389 g_{01}^+ (e_1 + e_2) + 2.6284 g_{02}^+ (e_3 + e_4), \quad (51)$$

where

$$\begin{aligned}
 e_1 &= \exp(-\alpha_1 \delta \eta) & e_3 &= \exp(-\alpha_2 \delta \eta) \\
 e_2 &= \exp(\alpha_1 \delta \eta) & e_4 &= \exp(\alpha_2 \delta \eta) \\
 b_o &= -\frac{1}{\sigma} [g_{01}^+ (e_1 + l_1 e_2 - e_2 - l_1 e_1 + \sigma e_2 + \sigma l_1 e_1) \\
 &\quad + g_{02}^+ (e_3 + l_2 e_4 - e_4 - l_2 e_3 + \sigma e_4 + \sigma l_2 e_3) \\
 &\quad + 0.1995 (2 - \sigma) + 0.0884 \sigma \delta] ,
 \end{aligned}$$

and g_{01}^+ and g_{02}^+ are determined by the solution of the following matrix equation

$$\begin{bmatrix} K_1 & K_2 \\ K_3 & K_4 \end{bmatrix} \begin{bmatrix} g_{01}^+ \\ g_{02}^+ \end{bmatrix} = \begin{bmatrix} 0.4680(2 - \sigma) \frac{1}{\delta} - 0.1507 \sigma \\ 0.1761 \frac{\sigma}{\delta} \end{bmatrix}$$

$$K_1 = [m_1 - (1 - \sigma)n_1]e_1 - [n_1 - (1 - \sigma)m_1]e_2$$

$$K_2 = [m_2 - (1 - \sigma)n_2]e_3 - [n_2 - (1 - \sigma)m_2]e_4$$

$$K_3 = [p_1 - (1 - \sigma)q_1]e_1 + [q_1 - (1 - \sigma)p_1]e_2$$

$$K_4 = [p_2 - (1 - \sigma)q_2]e_3 + [q_2 - (1 - \sigma)p_2]e_4$$

The volume flow rate is obtained by applying equation (33) to $q_z(\eta)$. The results of this integration are presented in Table 2, page 46, where $Q(\delta)$ is tabulated as a function of δ .

Iteration of the First Approximation. Equation (27) can be rewritten

as

$$\frac{dh^{*\pm}}{d\eta} + \frac{\delta}{c_x} h^{*\pm} = \frac{2\delta c_z}{c_x} q_z(\eta) - \frac{c_z}{c_x}. \quad (52)$$

Following the approach of Willis in reference 2, this equation is solved for $h^{*\pm}$. The solution is

$$h^{*\pm} = 2\delta \int_{\mp \frac{1}{2}}^{\eta} \frac{c_z}{c_x} q_z(\eta') e^{-(\eta-\eta')\delta/c_x} d\eta' - \int_{\mp \frac{1}{2}}^{\eta} \frac{c_z}{c_x} e^{-(\eta-\eta')\delta/c_x} d\eta', \quad (53)$$

where the integrating factor for equation (52) is $\exp(\eta\delta/c_x)$, and the constant of integration was found to be zero after applying the boundary condition $h^{*\pm}(\mp \frac{1}{2}) = 0$.

Using the definition of the velocity from equation (7), it is found that

$$q_z(\eta) = \frac{1}{2\sqrt{\pi}} \left\{ - \int_0^{\infty} \frac{1}{c_x} e^{-c_x^2} \left[2\delta \int_{\frac{1}{2}}^{\eta} q_z(\eta') e^{-(\eta-\eta')\delta/c_x} d\eta' - \int_{\frac{1}{2}}^{\eta} e^{-(\eta-\eta')\delta/c_x} d\eta' \right] dc_x + \int_0^{\infty} \frac{1}{c_x} e^{-c_x^2} \left[2\delta \int_{-\frac{1}{2}}^{\eta} q_z(\eta') e^{-(\eta-\eta')\delta/c_x} d\eta' - \int_{-\frac{1}{2}}^{\eta} e^{-(\eta-\eta')\delta/c_x} d\eta' \right] dc_x \right\}. \quad (54)$$

Equation (54) is in a form which requires a first guess for $q_2(\eta')$. Once this first guess is made, the first iteration of $q_2(\eta)$ can be calculated. This procedure can be carried out for any number of iterations. Furthermore, it is possible to show, in a manner similar to that presented by Willis (2), that the iteration is convergent.

Only one iteration is calculated here, and as a first guess the first approximation for the Krook model is used. Thus, for $\sigma = 1.0$,

$$q_2(\eta') = \frac{\pi}{4} \delta \eta'^2 - \frac{\pi}{16} \delta - \frac{\sqrt{\pi}}{4} .$$

After carrying out the integrations in equation (54) based on this first guess, the result is

$$\begin{aligned} q_2(\eta) = & \frac{\pi}{4} \delta \eta^2 - \frac{\pi}{16} \delta - \frac{\sqrt{\pi}}{4} - \frac{\sqrt{\pi}}{2\delta} [f_2(x_1) + f_2(x_2) - \frac{\sqrt{\pi}}{2}] \quad (55) \\ & - \frac{\sqrt{\pi}}{4} [f_1(x_1) + f_1(x_2)] + (\frac{1}{4} + \frac{1}{2\sqrt{\pi}\delta}) [f_1(x_1) + f_1(x_2) - \sqrt{\pi}] , \end{aligned}$$

where

$$f_m(x) = \int_0^{\infty} u^m e^{-u^2 - \frac{x}{u}} du \quad (56)$$

and $x_1 = (\frac{1}{2} - \eta)\delta$, $x_2 = (\eta + \frac{1}{2})\delta$. The integrals $f_m(x)$ are those defined by Abramowitz (23). The values of the integrals over the range of x were obtained from a Gauss-Hermite numerical quadrature (35). Since the quadrature method proved inaccurate for $x < 0.5$, the expansion used by Willis (24) for $x < 2.0$ was used. The accuracy of these methods is discussed in Chapter III.

After obtaining values for $q_z(\eta)$ at any number of specified points between the plates, the Simpson rule is used to obtain $Q(\delta)$ where

$$Q(\delta) = -2q_{z_{avg}} = -2 \int_{-\frac{1}{2}}^{\frac{1}{2}} q_z(\eta) d\eta . \quad (57)$$

The values of $Q(\delta)$ are tabulated in Table 3, page 50.

An asymptotic expression (independent of the initial guess of $q_z(\eta)$ for small δ) for $Q(\delta)$ for small δ is developed in Appendix E.

Hard Sphere Model

General

For the hard sphere model, the collision term of the Boltzmann equation is

$$\left(\frac{df}{dt}\right)_c = \int d^3v_1 \int_0^{2\pi} d\epsilon \int \frac{a^2}{4} \sin \theta d\theta v_r (f'f'_1 - ff_1) \quad (58)$$

where θ is the scattering angle, a is the molecular diameter, v_r is the relative velocity between molecules, and the "primes" denote the distribution function after collision. If it is assumed that $f = f_0(1+h^{*\pm})$, the Boltzmann equation becomes

$$c_x \frac{dh^{*\pm}}{d\eta} + c_z = \delta_s J(h^{*\pm}) , \quad (59)$$

where δ_s is the inverse Knudsen number for hard spheres defined as

$$\delta_s = dn_0 \sqrt{2} \pi a^2 , \quad (60)$$

and $J(h^{*\pm})$ is the collision term as a function of the perturbation which is defined by

$$J(h^{*\pm}) = \frac{1}{4\sqrt{2}\pi^{5/2}} \int e^{-\bar{c}_1^2} d^3c_1 \int_0^{2\pi} d\epsilon \int_0^\pi \sin\theta d\theta c_r \cdot (h^{*0} + h_1^{*0} - h^* - h_1^*) \quad (61)$$

The approach that is used to solve equation (59) differs slightly from that used in the previous section. Here, it will be assumed that

$$h^{*\pm} = c_z \sum_{i=0}^{n-1} a_i^\pm(\eta) c_x^i, \quad n = 1, 2, \dots \quad (62)$$

where n indicates the order of the approximation. Thus, for the first approximation, $n = 1$; for the second, $n = 2$, etc. In other words, $h^{*\pm}$ will not be developed in terms of orthogonal polynomials.

In the next two sections, the first and second approximations for the solution of the hard sphere model are presented. The first approximation, due to its brevity, is presented in full. The second approximation is presented in detail in Appendix F.

First Approximation

The perturbation of the distribution function assumes the form

$$h^{*\pm} = a_0^\pm(\eta) c_z \quad (63)$$

Following reference (19), it is possible to write the perturbation as

$$h^{*\pm} = \left(\frac{a_o^+ + a_o^-}{2} \right) c_z + \left(\frac{a_o^+ - a_o^-}{2} \right) c_z \text{ sign } c_x, \quad (64)$$

and

$$J(h^{*\pm}) = \left(\frac{a_o^+ + a_o^-}{2} \right) J(c_z) + \left(\frac{a_o^+ - a_o^-}{2} \right) J(c_z \text{ sign } c_x), \quad (65)$$

where

$$\text{sign } c_x \begin{cases} = +1, & c_x > 0 \\ = -1, & c_x < 0. \end{cases}$$

Multiply equation (59) by $c_z(1 \pm \text{sign } c_x)e^{-c_x^2}$ and integrate. The result is

$$\frac{d}{d\eta} a_o^\pm \pm \sqrt{\pi} = \delta_s \frac{I_1}{\pi} (a_o^+ - a_o^-), \quad (66)$$

where I_1 is called the bracket integral defined by

$$I = [A, B] = \int_{-\infty}^{+\infty} AJ(B) e^{-c^2} d^3c. \quad (67)$$

In this case

$$I_1 = [c_z \text{ sign } c_x, c_z \text{ sign } c_x]. \quad (68)$$

I_1 is a pure number and can always be calculated if the law of interaction for the molecules is known. Ziering, reference (25), clearly explains the use of the bracket integrals and carries out the integration of I_1 in detail. The velocities after collision can be determined by referring to Jeans, reference (26). If the center of mass coordinate system is used

(reference 27), in which

$$\bar{v}_c = \frac{\bar{c}}{2} + \frac{\bar{c}_1}{2}, \quad \bar{v}_r = \frac{\bar{c}}{2} - \frac{\bar{c}_1}{2}, \quad (69)$$

where \bar{v}_c is the velocity of the center of mass and \bar{v}_r is the relative velocity, the equations for the velocities after collision are

$$c'_{x_1} = v_{c_x} + \frac{v_{r_x}}{2} \cos \theta - \frac{1}{2} \sqrt{v_r^2 - v_{r_x}^2} \sin \theta \cos \epsilon \quad (70)$$

$$c'_{z_1} = v_{c_z} + \frac{v_{r_z}}{2} \cos \theta + \frac{1}{2} \frac{v_{r_x} x_{r_z}}{\sqrt{v_r^2 - v_{r_x}^2}} \sin \theta \cos \epsilon$$

$$+ \frac{1}{2} \frac{v_r v_{r_y}}{\sqrt{v_r^2 - v_{r_x}^2}} \sin \theta \sin \epsilon. \quad (71)$$

In the above equations, $v_r^2 = v_{r_x}^2 + v_{r_y}^2 + v_{r_z}^2$. In order to carry out the integration of the bracket integrals for the hard sphere model, it is most convenient to use cylindrical polar coordinates for \bar{v}_c and spherical coordinates for \bar{v}_r .

The solution of equation (66) for a_0^+ and a_0^- is straightforward. The velocity $q_z(\eta)$ is defined as in equation (7) and, for this first approximation, is equal to

$$q_z(\eta) = \frac{1}{4} (a_0^+ + a_0^-). \quad (72)$$

Since the first approximation does not yield suitable results, only the case $\sigma = 1$ is considered. For this case,

$$q_z(\eta) = -\frac{1}{2\sqrt{\pi}} \delta_s I_1 \eta^2 + \frac{1}{8\sqrt{\pi}} I_1 \delta_s - \frac{\sqrt{\pi}}{4} \quad (73)$$

and

$$Q(\delta_s) = -\frac{1}{6\sqrt{\pi}} I_1 \delta_s + \frac{\sqrt{\pi}}{2} . \quad (74)$$

The value of I_1 , first determined by Ziering (25) and checked for this work, is $I_1 = -1.0059 \pi$.

Second Approximation

For this case, the perturbation is assumed to be given by

$$h^{*\pm} = a_0^\pm c_z + a_1^\pm c_x c_z . \quad (75)$$

The details of the second approximation are presented in Appendix F. Consequently, only the results of this approximation are presented here.

The following bracket integrals are used in the second approximation,

$$I_2 = [c_z \text{ sign } c_x, c_z c_x] \quad (76)$$

$$I_3 = [c_z c_x, c_z c_x] \quad (77)$$

$$I_4 = [c_z c_x \text{ sign } c_x, c_z c_x \text{ sign } c_x] . \quad (78)$$

The values, which were first obtained by Ziering (25) and which were checked for this work, are

$$I_2 = -0.4345 \pi \quad (79)$$

$$I_3 = -0.4000 \pi \quad (80)$$

$$I_4 = -1.6982 \pi \quad (81)$$

The solution for the velocity is

$$\begin{aligned} q_z(\eta) = & \frac{1}{2} b_0 + 0.08179 \frac{1}{\delta_s} + 0.4508 \delta_s \eta^2 \\ & + \frac{1}{4} g_0^+ \left(1 + \ell + \frac{m-n}{\sqrt{\pi}} \right) (e_1 + e_2), \end{aligned} \quad (82)$$

where

$$e_1 = \exp(-\alpha \delta_s \eta) \quad e_2 = \exp(\alpha \delta_s \eta)$$

$$\alpha = 7.8598 \quad m = -1.5262$$

$$\ell = -4.3806 \quad n = -4.5452$$

$$\begin{aligned} b_0 = & \frac{1}{\sigma} \left\{ -0.03152(2 - \sigma) - 0.2254 \sigma \delta_s \right. \\ & \left. + g_0^+ \left[(\ell - 1)(e_1 - e_2) - \sigma(e_2 + \ell e_1) \right] \right\} \end{aligned} \quad (83)$$

$$g_0^+ = \frac{0.2899 (2 - \sigma) \frac{1}{\delta_s} + 0.9644 \sigma}{(n-m)(e_1 + e_2) + \sigma(me_2 - ne_1)} \quad (84)$$

The volume flow rate is

$$\begin{aligned} Q(\delta) = & -b_0 - 0.1636 \frac{1}{\delta_s} - 0.07513 \delta_s \\ & - \frac{1}{\alpha \delta_s} g_0^+ \left(1 + \ell + \frac{m-n}{\sqrt{\pi}} \right) \left(e^{\alpha \delta_s / 2} - e^{-\alpha \delta_s / 2} \right). \end{aligned} \quad (85)$$

$Q(\delta_s)$ versus δ_s is tabulated in Table 4, page 55.

Maxwellian Model

General

The only major difference in the development of the solution for the Maxwellian model compared to the hard sphere model is the evaluation of the bracket integrals. Otherwise, the basic equation is

$$c_x \frac{dh^{*\pm}}{d\eta} + c_z = \delta_m J(h^{*\pm}) \quad (86)$$

where $\delta_m = dn_0 \cdot 6 \sqrt{\pi} A_2(5) \sqrt{R_1/kT}$ and

$$J(h^{*\pm}) = \frac{1}{6\pi^2 A_2(5)} \sqrt{\frac{m}{2R_1}} \int e^{-\frac{c^2}{2}} d^3c_1 \int_0^{2\pi} d\varepsilon \int_0^\pi \sin\theta F(\theta, R_1) d\theta \cdot [h_1^{*+} + h^{*+} - h_1^{*-} - h^{*-}] \quad (87)$$

$A_2(5)$ is a pure number, evaluated by Maxwell (36), equal to 0.436. R_1 is the force constant for the inverse force law,

$$\text{Force} = \frac{R_1}{r^5} \quad (88)$$

which Maxwell molecules obey. $F(\theta, R_1)$ is a function of the scattering angle such that

$$F(\theta, R_1) = \sqrt{\frac{m}{2R_1}} v_r \cdot I(v_r, \theta)$$

where v_r is the relative velocity between two colliding molecules and $I(v_r, \theta)$ is the scattering cross section.

Three approximations for the Maxwellian model are calculated. The bracket integrals I_1 , I_2 , I_3 , and I_4 have been previously calculated by Ziering (21), and have been checked for this work. The values are

$$\begin{aligned} I_1 &= -2.31875 \\ I_2 &= -0.696041 \\ I_3 &= -0.616850 \\ I_4 &= -0.318338 . \end{aligned}$$

The bracket integrals I_1 and I_4 must be calculated by a numerical scheme. It is possible to carry out all of the integrations except the integration over θ . After integrating over all variables except θ , I_1 and I_4 can be written in the form

$$I_i = \frac{1}{6\pi^2 A_2(5)} \sqrt{\frac{m}{2R_1}} \int_0^\pi \sin \theta F(\theta, R_1) G_i(\theta) d\theta \quad (89)$$

where $G_i(\theta)$ is different for each bracket integral. Following Wang Chang and Uhlenbeck (28),

$$F(\theta, R_1) \sin \theta d\theta = \sqrt{\frac{m}{2R_1}} v_r b db, \quad (90)$$

where b is the impact parameter in a binary collision. By defining $\alpha = (mv_r^2/2R_1)^{1/4} b$, equation (90) can be rewritten as

$$\sqrt{\frac{m}{2R_1}} F(\theta, R_1) \sin \theta d\theta = \alpha d\alpha. \quad (91)$$

If the substitution $\alpha^4 = 2 \cot 2\varphi$ is made, then

$$\sqrt{\frac{m}{2R_1}} F(\theta, R_1) \sin \theta d\theta = -\sqrt{2} \frac{1}{\sin^2 2\phi} d\phi. \quad (92)$$

From the collision dynamics (26), it is known that

$$\theta = \pi - 2 \sqrt{\cos 2\phi} K(\sin \phi), \quad (93)$$

where

$$K(\sin \phi) = \int_0^{\pi/2} \frac{d\psi}{\sqrt{1 - \sin^2 \phi \sin^2 \psi}} \quad (94)$$

is the complete elliptic integral of the first kind. Using equation (92) in equation (89), the bracket integrals become

$$I_i = \frac{1}{6\pi^2 A_2(\delta)} \int_0^{\pi/4} \frac{G_i(\theta)}{\sin^2 2\phi} d\theta.$$

The expression $G_i(\theta)$ can be calculated for any ϕ using equation (93). The values for I_i , which were found numerically, were obtained by using the Simpson rule.

First Approximation

Following the development for the hard sphere model, the velocity, where $\sigma = 1.0$, is given by

$$q_z(\eta) = -\frac{1}{2\sqrt{\pi}} \delta_m^{-1} \eta^2 + \frac{1}{8\sqrt{\pi}} I_1 \delta_m - \frac{\sqrt{\pi}}{4}. \quad (95)$$

Also, the volume flow rate is

$$Q(\delta_m) = -\frac{1}{6\sqrt{\pi}} I_1 \delta_m + \frac{\sqrt{\pi}}{2}. \quad (96)$$

Second Approximation

The method of solution is identical to that presented in Appendix F, where only the values of the bracket integrals change. The solution for the velocity is

$$q_z(\eta) = \frac{1}{2} b_o + 1.3920 \frac{1}{\delta_m} + 0.2216 \delta_m \eta^2 + \frac{1}{4} g_o^+ (1 + \ell + \frac{m-n}{\sqrt{\pi}}) (e_1 + e_2), \quad (97)$$

where

$$e_1 = \exp(-\alpha \delta_m \eta) \quad e_2 = \exp(\alpha \delta_m \eta)$$

$$\alpha = 1.8368 \quad m = -0.7222$$

$$\ell = 2.3546 \quad n = 2.2507$$

$$b_o = \frac{1}{\sigma} \left\{ -0.1108 \sigma \delta_m + g_o^+ [(\ell-1)(e_1 - e_2) - \sigma(e_2 + \ell e_1)] \right\}$$

$$g_o^+ = \frac{4.9345(2 - \sigma) \frac{1}{\delta_m} + 1.0000 \sigma}{(n-m)(e_1 + e_2) + \sigma(m e_2 - n e_1)} .$$

The volume flow rate is

$$Q(\delta_m) = -b_o - 2.7839 \frac{1}{\delta_m} - 0.03693 \delta_m - \frac{1}{\alpha \delta_m} g_o^+ (1 + \ell + \frac{m-n}{\sqrt{\pi}}) (e^{\alpha \frac{\delta_m}{2}} - e^{-\alpha \frac{\delta_m}{2}}) . \quad (98)$$

The tabulated values of $Q(\delta_m)$ versus δ_m are presented in Table 5, page 62.

Third Approximation

In this case,

$$h^{*\pm} = (a_0^\pm + a_1^\pm c_x + a_2^\pm c_x^2) c_z \quad (99)$$

The moment equations are obtained in a manner similar to that used in the second approximation. The three basic differential equations are

$$\begin{aligned} \frac{da_0^\pm}{d\eta} \pm \frac{\sqrt{\pi}}{2} \frac{da_1^\pm}{d\eta} + \frac{da_2^\pm}{d\eta} \pm \sqrt{\pi} = \frac{1}{\pi} [I_2(a_1^+ + a_1^-) + I_1(a_0^+ - a_0^-) \\ + I_8(a_2^+ - a_2^-)] \quad (100) \end{aligned}$$

$$\begin{aligned} \frac{da_0^\mp}{d\eta} \pm \frac{2}{\sqrt{\pi}} \frac{da_1^\mp}{d\eta} + \frac{3}{2} \frac{da_2^\mp}{d\eta} \pm \frac{2}{\sqrt{\pi}} = \frac{2}{\pi\sqrt{\pi}} [I_3(a_1^+ + a_1^-) \\ + I_2(a_0^+ - a_0^-) + I_6(a_2^+ - a_2^-) \pm I_5(a_2^+ + a_2^-) \pm I_4(a_1^+ - a_1^-)] \quad (101) \end{aligned}$$

$$\begin{aligned} \frac{da_0^\mp}{d\eta} \pm \frac{3\sqrt{\pi}}{4} \frac{da_1^\mp}{d\eta} + 2 \frac{da_2^\mp}{d\eta} \pm \frac{\sqrt{\pi}}{2} = \frac{1}{\pi} [\pm I_7(a_2^+ + a_2^-) \\ \pm I_5(a_1^+ - a_1^-) + I_6(a_1^+ + a_1^-) + I_8(a_0^+ - a_0^-) + I_9(a_2^+ - a_2^-)] \quad (102) \end{aligned}$$

The five additional bracket integrals are defined as

$$\begin{aligned} I_5 &= [c_z c_x \text{ sign } c_x, c_z c_x^2] \\ I_6 &= [c_z c_x^2 \text{ sign } c_x, c_z c_x] \\ I_7 &= [c_z c_x^2, c_z c_x^2] \\ I_8 &= [c_z c_x^2 \text{ sign } c_x, c_z \text{ sign } c_x] \\ I_9 &= [c_z c_x^2 \text{ sign } c_x, c_z c_x^2 \text{ sign } c_x]. \end{aligned}$$

I_8 and I_9 must be calculated numerically in the same manner as I_1 and

I_4 . See Appendix G for the calculation of I_8 (the calculation of I_9 is similar). Their values are

$$I_5 = -0.464027$$

$$I_6 = -0.696041$$

$$I_7 = -0.822467$$

$$I_8 = -0.49656$$

$$I_9 = -0.8530 .$$

The solution of the determinant of the coefficient matrix for the homogeneous set of equations yields $\alpha_1 = 0.1338$ and $\alpha_2 = 4.5108$. The solution for the velocity is

$$\begin{aligned} q_z(\eta) = & \frac{1}{2} b_0 + \frac{1}{2} b_2 \delta_m \eta^2 + \frac{1}{2\sqrt{\pi}} \frac{b_4}{\delta_m} + \frac{1}{4} \frac{b_8}{\delta_m} + \frac{g_{01}^+}{4} (1 + \ell_1 \\ & + \frac{m_1 - n_1}{\sqrt{\pi}} + \frac{p_1 + q_1}{2})(e_2 + e_1) + \frac{g_{02}^+}{4} (1 + \ell_2 \\ & + \frac{m_2 - n_2}{\sqrt{\pi}} + \frac{p_2 + q_2}{2})(e_4 + e_3) , \end{aligned} \quad (103)$$

where

$$e_1 = \exp(-\alpha_1 \delta_m \eta) \quad e_3 = \exp(-\alpha_2 \delta_m \eta)$$

$$e_2 = \exp(\alpha_1 \delta_m \eta) \quad e_4 = \exp(\alpha_2 \delta_m \eta)$$

$$\ell_1 = -0.3857 \quad \ell_2 = 2.9984$$

$$m_1 = -4.0726 \quad m_2 = -1.5340$$

$$n_1 = -6.1927 \quad n_2 = 5.7021$$

$$p_1 = -2.8537 \quad p_2 = 0.5411$$

$$q_1 = -4.8581 \quad q_2 = 2.2366$$

$$b_o = \frac{1}{2} b_1 + \frac{b_2}{4} \delta_m - g_{01}^+ (e_1^o + l_1 e_2^o) - g_{02}^+ (e_3^o + l_2 e_4^o)$$

$$g_{01}^+ = \left[\left(\frac{1}{2} b_5 - \frac{b_4}{\delta_m} \right) (p_2 e_3^o + q_2 e_4^o) - \left(\frac{1}{2} b_9 - \frac{b_8}{\delta_m} \right) (m_2 e_3^o - n_2 e_4^o) \right] / K_1$$

$$g_{02}^+ = \left[\left(\frac{1}{2} b_9 - \frac{b_8}{\delta_m} \right) (m_1 e_1^o - n_1 e_2^o) - \left(\frac{1}{2} b_5 - \frac{b_4}{\delta_m} \right) (p_1 e_1^o + q_1 e_2^o) \right] / K_1$$

$$K_1 = (m_1 e_1^o - n_1 e_2^o) (p_2 e_3^o + q_2 e_4^o) - (m_2 e_3^o - n_2 e_4^o) (p_1 e_1^o + q_1 e_2^o)$$

$$e_1^o = \exp(-\alpha_1 \delta_m / 2) \quad e_3^o = \exp(-\alpha_2 \delta_m / 2)$$

$$e_2^o = \exp(\alpha_1 \delta_m / 2) \quad e_4^o = \exp(\alpha_2 \delta_m / 2)$$

$$b_1 = 0.00001 \quad b_5 = -2.0001$$

$$b_2 = 0.00044 \quad b_8 = 3.3850$$

$$b_4 = 0.00013 \quad b_9 = 0.00006$$

The volume flow rate is

$$\begin{aligned}
Q(\delta_m) = & b_0 - \frac{1}{\sqrt{\pi}} b_4 \frac{1}{\delta_m} - \frac{1}{2} b_8 \frac{1}{\delta_m} - \frac{1}{12} b_{12} \delta_m + g_{01}^+ (1 + \ell_1 \\
& + \frac{m_1 - n_1}{\sqrt{\pi}} + \frac{p_1 + q_1}{2}) (e_1^i - e_2^i) + g_{02}^+ (1 + \ell_2 \\
& + \frac{m_2 - n_2}{\sqrt{\pi}} + \frac{p_2 + q_2}{2}) (e_3^i - e_4^i) .
\end{aligned} \tag{109}$$

Values of the volume flow rate as a function of δ_m are tabulated in Table 6, page 63.

CHAPTER III

DISCUSSION OF RESULTS

Experimental Data

The earliest experimental work available is that of Gaede (9), carried out in 1913. Since the accuracy of the data is uncertain and since the results disagree considerably with the two later sets of data, Gaede's work is not included in the comparison of experimental data and theoretical results.

The data collected by Rasmussen in 1937 (11) are more reliable and are used in this study to evaluate the theoretical results. Rasmussen measured the flow rate between two glass plates, 1.82×10^{-3} cm. apart. The width of the slit was 1.32 cm., and the dimension in the direction of flow was 0.963 cm. His apparatus consisted of two tanks each connected to one end of the glass plates. McLeod gauges and manometers were connected to each tank. Knowing the volume of the tanks and the time it took for the gas to flow from one tank (at a specified pressure) to the other tank, Rasmussen was able to calculate the average volume flow rate. If Q_r is the volume flow rate, t_1 is the initial time, t_2 is the final time, ()^v denotes the conditions in the first tank, and ()^{''} denotes the conditions in the second tank, then the volume flow rate observed by Rasmussen was found by the following equation:

$$Q_r = \frac{l}{t_2 - t_1} \left(\frac{V^v V''}{V^v + V''} \right) \ln \left(\frac{P_1^v - P_2^v}{P_1'' - P_2''} \right) .$$

Rasmussen used only hydrogen in his experiments with parallel plates. The mean free path and volume flow rate used by Rasmussen have been converted to the corresponding quantities calculated in the theoretical analysis of this dissertation. The results are plotted in Figure 4.

The latest available experimental data is that of Dong (4), completed in 1956. His apparatus consisted of two parallel steel plates, 0.324 cm. apart. The width of the slit was 22.86 cm. The inlet and exit were 127.00 cm. apart; however, the initial pressure tap and final pressure tap were 61.0 cm. apart, located 33.0 cm. from the inlet and exit, respectively. After introducing the gas into the system, the moisture was removed, and the gas was passed through a heat exchanger. Then, after passing across two flowmeters, the gas entered the test section through a series of needle valves. The pressure was measured at two points along the axis of the test section by McLeod gauges. A pumping unit was connected to the exit of the test section. Dong measured his volume flow rate by increasing the pressure in the system to a predetermined value, closing the system, and allowing the gas to pass from the flowmeter through the test section. The time for the pressure in the flowmeter to change from the predetermined value to the final value was then recorded. From this information he calculated the volume flow rate. Dong carried out his experiments with the gases H_2 , He, air, CO_2 , and freon-12.

There is some disagreement between Dong's and Rasmussen's data in the transition and near-free-molecular regions. The disagreement in the near-free-molecular region can most likely be attributed to the experimental apparatus. Rasmussen's apparatus more closely approximates the infinite parallel plate geometry. For this reason, Rasmussen's data are probably

to be preferred in the near-free-molecular region. Furthermore, in his paper, Rasmussen calculated the free-molecular value for the volume flow rate for a three-dimensional channel (using an equation developed by Clausing). He found this limiting value to be thirty percent higher than his maximum observed value, and attributed the difference to the geometry of his apparatus.

On the other hand, Dong's data might be preferred when comparing experiment and theory because of his location of pressure taps. By locating the pressure taps out of the region of the end effects, Dong's data should furnish better agreement with the theory, since the theoretical development is based upon the assumption of constant pressure gradient. The validity of this idea is established in Figures 2, 3, and 4.

Although Dong's data indicate a small variation in minimum values of the volume flow rate for different gases, this minimum effect is better illustrated by the experimental work of Hanley and Steele (29) in 1964. Their work, although carried out for long tubes, shows very clearly the effect of the gas on the minimum volume flow rate. The trend of their data is the same as Dong's; however, a comparison cannot be made because of the different geometries.

Krook Model

Full-Range Method

Even before results are available for the solution by the full-range method, it is not expected that the solution will adequately describe the velocity moments in the near-free-molecular flow regime. This is because the full-range method does not exactly specify the molecular boundary conditions, which require that the distribution function be discontinuous

at the walls. That is, for the near-free-molecular flow, the distribution function should be explicitly divided into two streams. This belief is validated by the results of the first, second, and third approximations shown in Figure 2.

The volume flow rate for the first approximation is obtained from equation (20); for the second approximation, equation (23). The tabulated values of the volume flow rate for the third approximation are given in Table 1. Also, Cercignani's numerical solution of equation (6) is presented. If the polynomial approximation is correct, it should converge to Cercignani's results, as it does. Dong's results for helium are also plotted in Figure 2 to indicate the comparison with experimental data. Since neither the first, second, or third approximations show a minimum in the transition regime, no higher approximations were carried out. The results of similar work using the full-range method for Couette flow (1) also indicate a slow convergence, and it was not considered worthwhile to pursue the solution by this method.

Half-Range Method

From the experience of previous investigators using the half-range method (1) (19) (20) (21), it is expected that, for the same approximation, a better solution will be obtained by this method than by the full-range method. That this is so, is seen in Figure 3. The volume flow rate for the first approximation is obtained from equation (44); the second approximation, from equation (47). The volume flow rate for the third approximation is obtained from equation (51), tabulated in Table 2, and plotted in Figure 3. Cercignani's numerical results are also presented in Figure 3 to illustrate the convergence of the solution by the polynomial approximation

Table 1. Volume Flow Rate Versus Inverse Knudsen Number
for the Third Approximation by the Full-Range
Method for the Krook Model

δ	Q	δ	Q
0.01	1.4090	1.70	1.5360
0.05	1.4090	1.80	1.5473
0.10	1.4092	1.90	1.5588
0.20	1.4112	2.00	1.5706
0.30	1.4146	2.50	1.6318
0.40	1.4193	3.00	1.6966
0.50	1.4250	3.50	1.7644
0.60	1.4315	4.00	1.8345
0.70	1.4388	5.00	1.9799
0.80	1.4467	6.00	2.1306
0.90	1.4551	7.00	2.2846
1.00	1.4640	8.00	2.4412
1.10	1.4734	9.00	2.5995
1.20	1.4831	10.00	2.7591
1.30	1.4931	15.00	3.5692
1.40	1.5034	20.00	4.3894
1.50	1.5140	25.00	5.2143
1.60	1.5249	30.00	6.0418

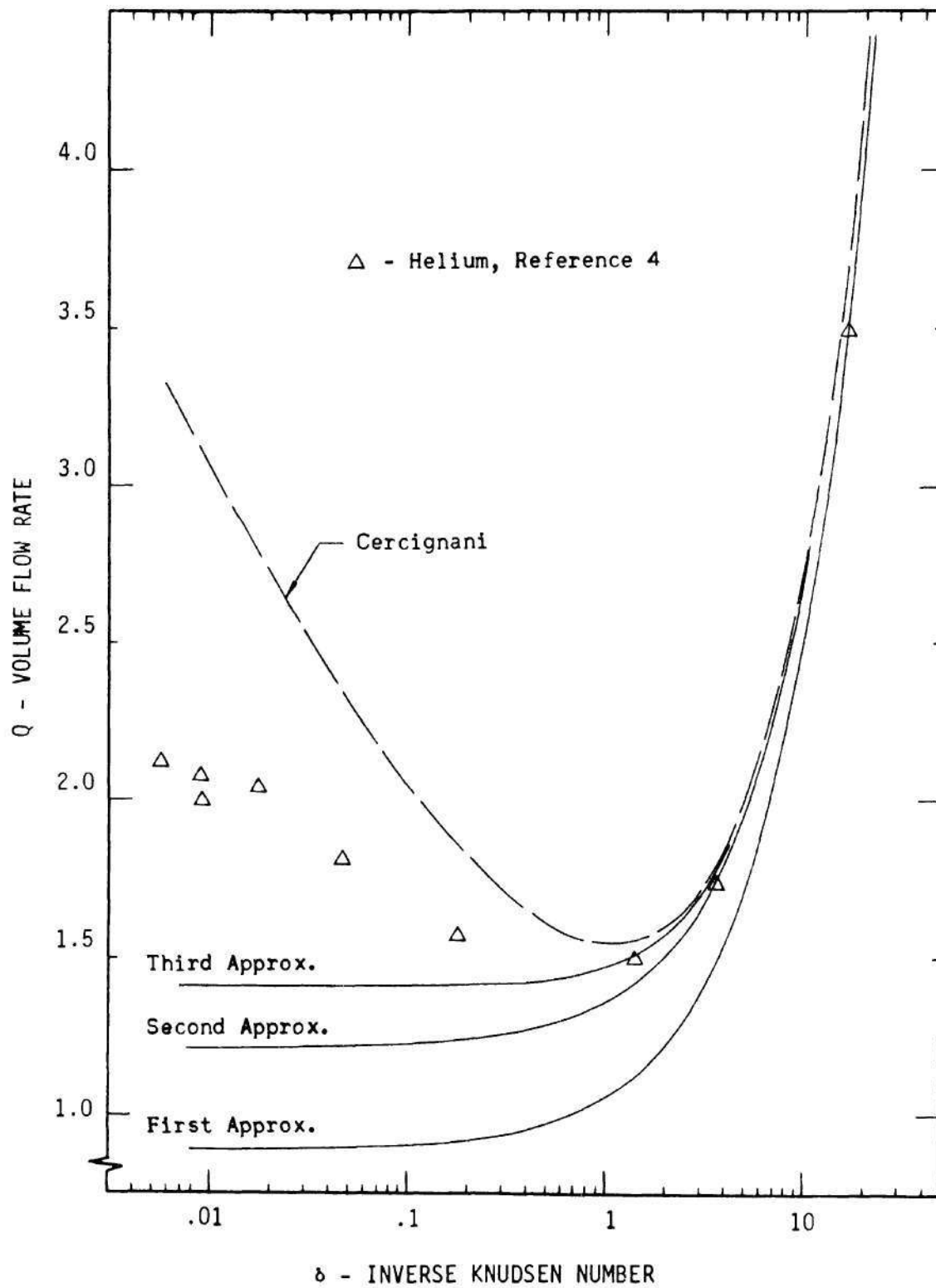


Figure 2. Volume Flow Rate versus Inverse Knudsen Number for the Krook Model, Full-Range Moment Method.

Table 2. Volume Flow Rate Versus Inverse Knudsen Number
for the Third Approximation by the Half-Range
Method for the Krook Model

δ	Q	δ	Q
0.01	1.5993	1.70	1.5864
0.05	1.6035	1.80	1.5930
0.10	1.6066	1.90	1.6004
0.20	1.6076	2.00	1.6084
0.30	1.6039	2.50	1.6567
0.40	1.5979	3.00	1.7146
0.50	1.5910	3.50	1.7787
0.60	1.5842	4.00	1.8469
0.70	1.5782	5.00	1.9910
0.80	1.5733	6.00	2.1413
0.90	1.5698	7.00	2.2954
1.00	1.5675	8.00	2.4519
1.10	1.5667	9.00	2.6101
1.20	1.5672	10.00	2.7696
1.30	1.5689	15.00	3.5789
1.40	1.5717	20.00	4.3985
1.50	1.5757	25.00	5.2231
1.60	1.5806	30.00	6.0503

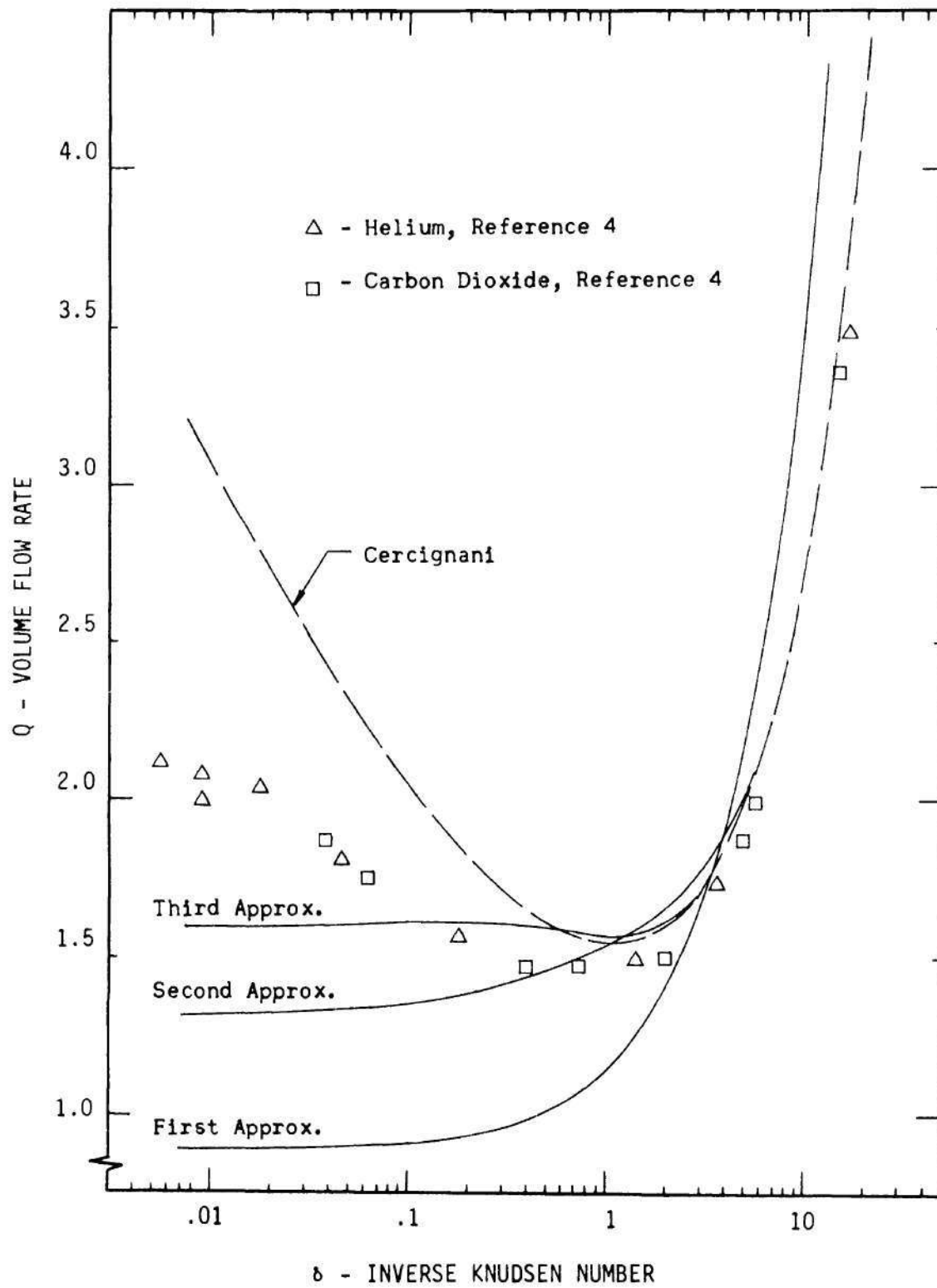


Figure 3. Volume Flow Rate versus Inverse Knudsen Number for the Krook Model, Half-Range Moment Method.

method to his results.

As seen in the figure, the third approximation successfully yields the desired minimum in the transition region. Because the convergence of the half-range method is very slow in the near-free-molecular region, the third approximation exhibits a relative maximum at $\delta \cong 0.20$. This maximum occurs because the convergence is somewhat faster in the transition region than in the free-molecular region. The reason for the slow convergence is that the free-molecular limit has a non-analytic character, as shown by Cercignani (16), which cannot be adequately represented by a finite number of terms in a polynomial approximation. This has been pointed out by Gross and Jackson in reference 30.

In addition to the theoretical results presented in Figure 3, Dong's data for helium and carbon dioxide are presented. His data for the other gases differ little from that presented.

It is possible to obtain the free-molecular value for the volume flow rate by solving the basic moment equations for each approximation where δ is set equal to zero. This is equivalent to setting the collision integral equal to zero, which is the case for free-molecular flow. The results of this procedure are

$$\lim_{\delta \rightarrow 0} Q = 0.886 \quad (\text{first})$$

$$\lim_{\delta \rightarrow 0} Q = 1.314 \quad (\text{second})$$

$$\lim_{\delta \rightarrow 0} Q = 1.598 \quad (\text{third})$$

As an extension of this idea, it is seen that these are also the limiting values for any other molecular model since the law of interaction for free-molecular flow cannot affect the flow properties.

The behavior in the continuum region is exhibited by the following limits:

$$\lim_{\delta \rightarrow \infty} Q = 0.2618 \delta + 0.8862 \quad (\text{first})$$

$$\lim_{\delta \rightarrow \infty} Q = 0.1667 \delta + 1.0209 \quad (\text{second})$$

$$\lim_{\delta \rightarrow \infty} Q = 0.1667 \delta + 1.0170 \quad (\text{third}).$$

The convergence of the solution in the continuum region is very fast, the solution being essentially correct in the second approximation.

Cercignani (3) found

$$\lim_{\delta \rightarrow \infty} Q = 0.1667 \delta + 1.0161$$

for his numerical results.

Iteration Method

The results of the numerical integration of equation (55) to find the volume flow rate are tabulated in Table 3 and plotted in Figure 4. Cercignani's numerical results and the data from Dong's paper for helium and carbon dioxide are also presented. In addition, Rasmussen's results for hydrogen are included.

In order to integrate equation (55), it was necessary to know the integrals $f_m(x)$ for any x . It is possible to use Abramowitz's work to

Table 3. Volume Flow Rate Versus Inverse Knudsen Number
for the First Iteration of the Krook Model by
the Willis Method

δ	Q	δ	Q
0.0001	5.5552	1.30	1.3290
0.001	4.2592	1.40	1.3433
0.01	2.9856	1.50	1.3590
0.02	2.6173	1.60	1.3759
0.03	2.4088	1.70	1.3939
0.04	2.2652	1.80	1.4128
0.05	2.1569	1.90	1.4325
0.06	2.0706	2.00	1.4529
0.07	1.9995	2.50	1.5621
0.08	1.9394	3.00	1.6795
0.09	1.8877	3.50	1.8017
0.10	1.8425	4.00	1.9268
0.20	1.5755	4.50	2.0539
0.30	1.4508	5.00	2.1822
0.40	1.3806	6.00	2.4411
0.50	1.3388	7.00	2.7017
0.60	1.3140	8.00	2.9632
0.70	1.3003	9.00	3.2252
0.80	1.2945	10.00	3.4874
0.90	1.2944	15.00	4.7992
1.00	1.2987	20.00	6.1106
1.10	1.3063	25.00	7.4213
1.20	1.3166	30.00	8.7315

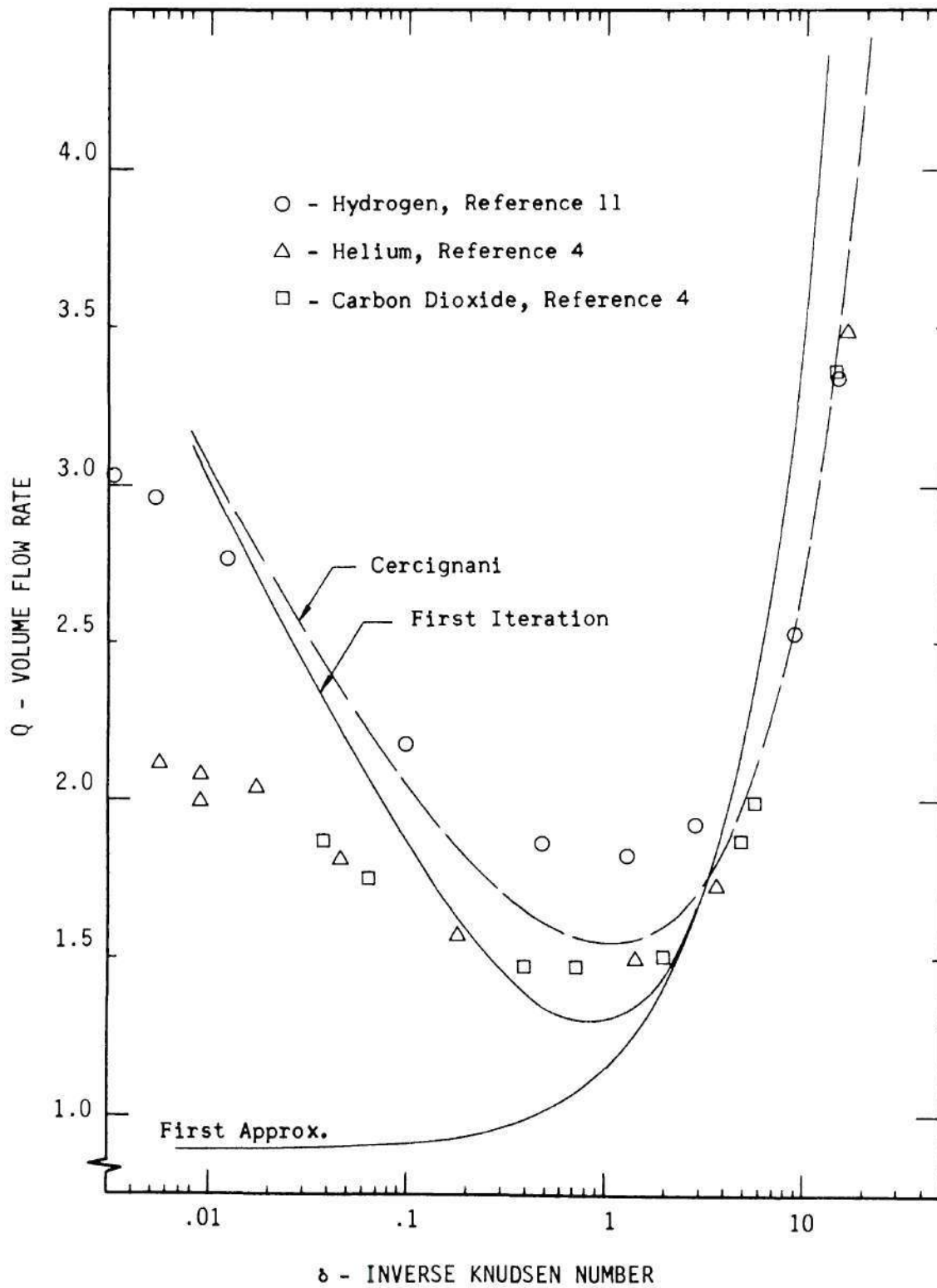


Figure 4. Volume Flow Rate versus Inverse Knudsen Number for the Krook Model, Willis Iteration Method.

find asymptotic expressions for all $f_m(x)$ for large x and small x , but this does not give a complete solution over the entire Knudsen number range. Consequently, the Gauss-Hermite numerical quadrature was used. The method is described by equation (25.4.46) of the Handbook of Mathematical Functions (31), and the zeros of the Hermite polynomials are tabulated to fifteen decimal places on page 924 of the same reference. Because the quadrature method is accurate to only two decimal places for $x < 10^{-3}$ for the integral $f_0(x)$, the more accurate method presented by Willis (24) was used for $x \leq 2.0$. He used an expansion of the form

$$f_m(x) = g_1 + (x \ln x) g_2$$

where g_1 and g_2 are polynomials depending on m , and are obtained from Abramowitz's work. Willis tabulates the g_1 and g_2 , and the accuracy of the expansion is such that the error is less than 1×10^{-6} .

As shown in Appendix E, the asymptote for $\delta \rightarrow 0$ is given by

$$\lim_{\delta \rightarrow 0} Q = \frac{1}{2\sqrt{\pi}} - \frac{1}{2\sqrt{\pi}} \ln \delta ,$$

no matter what approximation is used as a first guess for the iteration.

The satisfactory results of the iteration method are due to the introduction of the non-analytic behavior of $f_0(x)$ for small x . It is this integral which dominates the behavior of $Q(\delta)$ for small δ .

The results of the iteration method, shown in Figure 4, indicate that the solution is satisfactory for all of the flow regimes, from free-molecular to continuum. As explained earlier, Rasmussen's data (11) is preferred for the free-molecular region, and Dong's data (4) is preferred

for the transition region. The iteration method agrees closely with the trend of the preferred data.

Although it is true mathematically that the correct solution of the Boltzmann equation for this one-dimensional problem indicates an infinite limit for $\delta \rightarrow 0$, it is felt that if the two-dimensional problem were considered (i.e., include the z-dependent terms in the solution) a finite limit for $Q(\delta)$ would be obtained as $\delta \rightarrow 0$. After considering that the volume flow rate for an infinite length tube is finite as $\delta \rightarrow 0$, it is reasonable to expect the volume flow rate (based on a unit width of the slit) for the parallel plates be finite as $\delta \rightarrow 0$. This problem is presently being investigated by using the discrete ordinate method (35).

Hard Sphere Model

Although Dong's data are used in a comparison with the theory, it is necessary to calculate the inverse Knudsen number based on the hard sphere model. For hard spheres $\delta_s = dn_0 \sqrt{2} \pi a^2$. n_0 can be written as p/kt , where the average pressure between the two pressure taps is used. Thus, $\delta_s = dpa^2 \sqrt{2} \pi / kT$. The plate separation distance is 0.324 cm., $T \approx 296$ °K for all experiments, and k is Boltzmann's constant. Thus, $\delta_s = 4.700 \times 10^{-3} pa^2$ where p is the average pressure measured in microns, and a is the molecular diameter measured in Angstrom units.

The average pressure is obtained from Dong's tabulations of each experiment run. The molecular diameter can be obtained from the calculation of the viscosity coefficient based on the hard sphere model. The derived relation is (reference 38)

$$\eta \times 10^7 = 266.93 \frac{\sqrt{M} \sqrt{T}}{a^2},$$

where η is measured in gm/cm-sec, M is the molecular weight, T is the temperature in $^{\circ}\text{K}$, and a is the molecular diameter measured in Angstrom units. Using the data in reference 32 for viscosity yields

$$a_{\text{H}_2} = 2.721 \text{ \AA}$$

$$a_{\text{He}} = 2.170 \text{ \AA}$$

$$a_{\text{CO}_2} = 4.524 \text{ \AA} .$$

Thus, it is possible to calculate δ_s for each experiment in Dong's work.

The volume flow rate for the first approximation is obtained from equation (74), the second approximation, from equation (85). $Q(\delta)$ is tabulated in Table 4 for the second approximation. The results for the first and second approximations are plotted in Figures 5, 6, and 7 for hydrogen, helium, and carbon dioxide, respectively.

As seen in each of Figures 5, 6, and 7, the second approximation presents the desired minimum in the transition region. The minimum is apparently well-placed with respect to the experimental data. Furthermore, the results in the continuum region exhibit very good agreement with the data. The results also indicate that the half-range moment method, applied to the hard sphere model, can suitably differentiate between gases.

Cercignani (33) has raised an objection to the solution of the Boltzmann equation with the hard sphere model by the half-range moment method. That is, it is expected that the half-range character of the distribution function will be destroyed away from the wall. For this to occur he shows that the ratio I_2/I_3 must equal 1.128. For the hard

Table 4. Volume Flow Rate Versus Inverse Knudsen Number
for the Second Approximation by the Half-Range
Method for the Hard Sphere Model

δ	Q	δ	Q
0.01	1.2922	0.90	1.1581
0.02	1.2731	1.00	1.1684
0.03	1.2565	1.50	1.2275
0.04	1.2420	2.00	1.2934
0.05	1.2293	2.50	1.3627
0.06	1.2181	3.00	1.4338
0.07	1.2082	3.50	1.5060
0.08	1.1994	4.00	1.5788
0.09	1.1916	5.00	1.7259
0.10	1.1846	6.00	1.8739
0.20	1.1438	7.00	2.0226
0.30	1.1295	8.00	2.1717
0.40	1.1261	9.00	2.3210
0.50	1.1281	10.00	2.4705
0.60	1.1331	15.00	3.2194
0.70	1.1402	20.00	3.9696
0.80	1.1486	25.00	4.7201

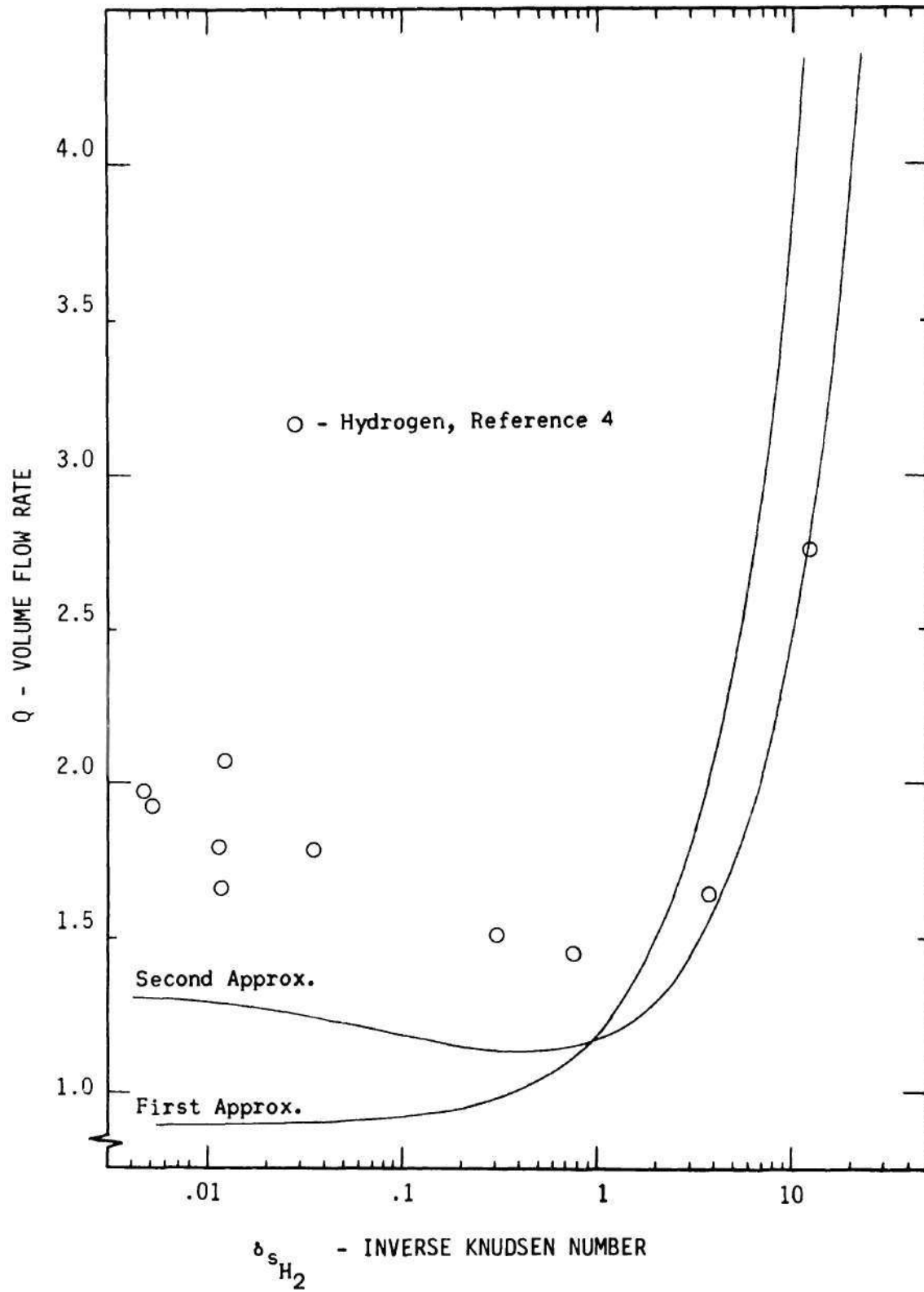


Figure 5. Volume Flow Rate versus Inverse Knudsen Number for the Hard Sphere Model, Hydrogen.

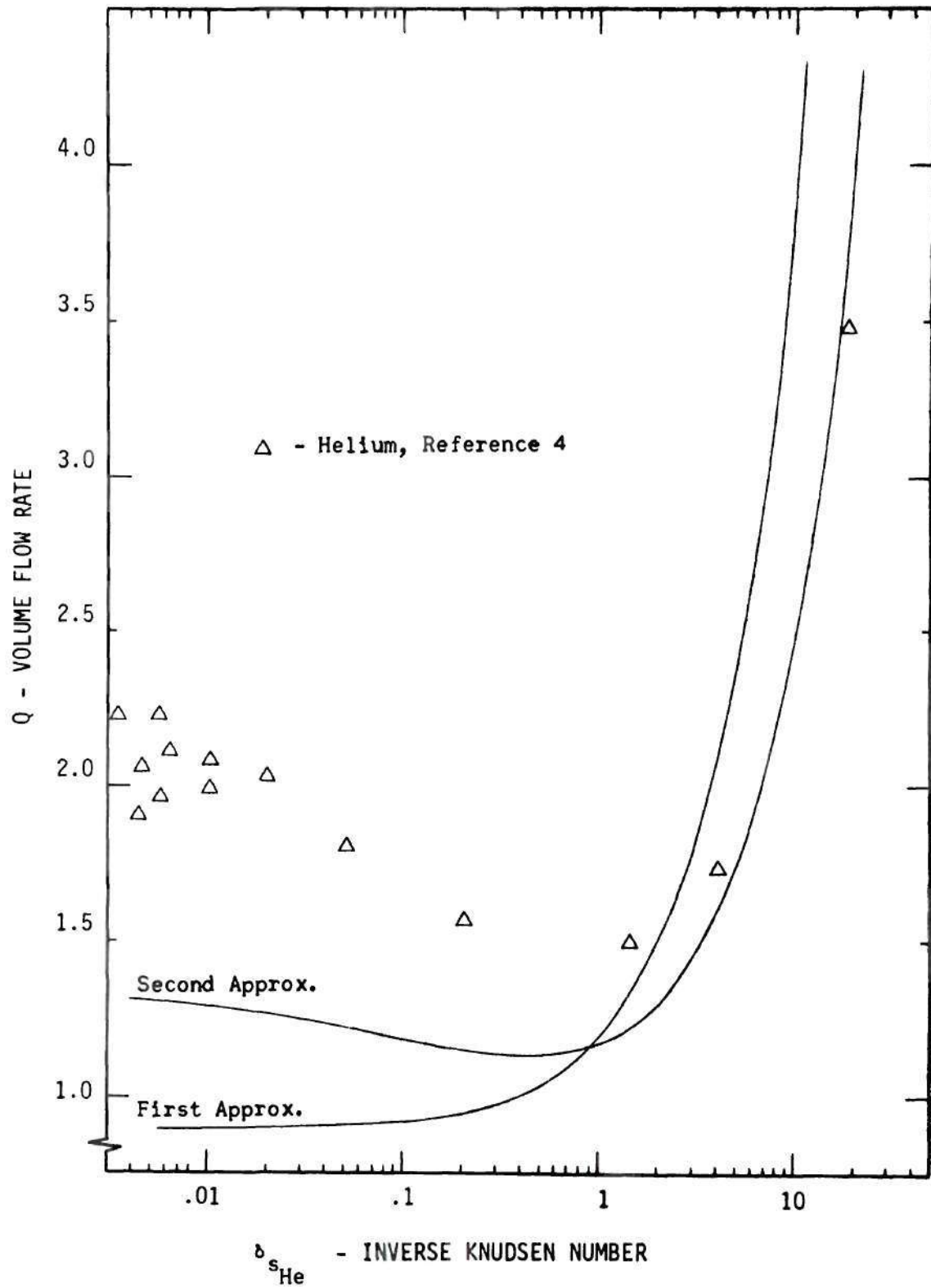


Figure 6. Volume Flow Rate versus Inverse Knudsen Number for the Hard Sphere Model, Helium.

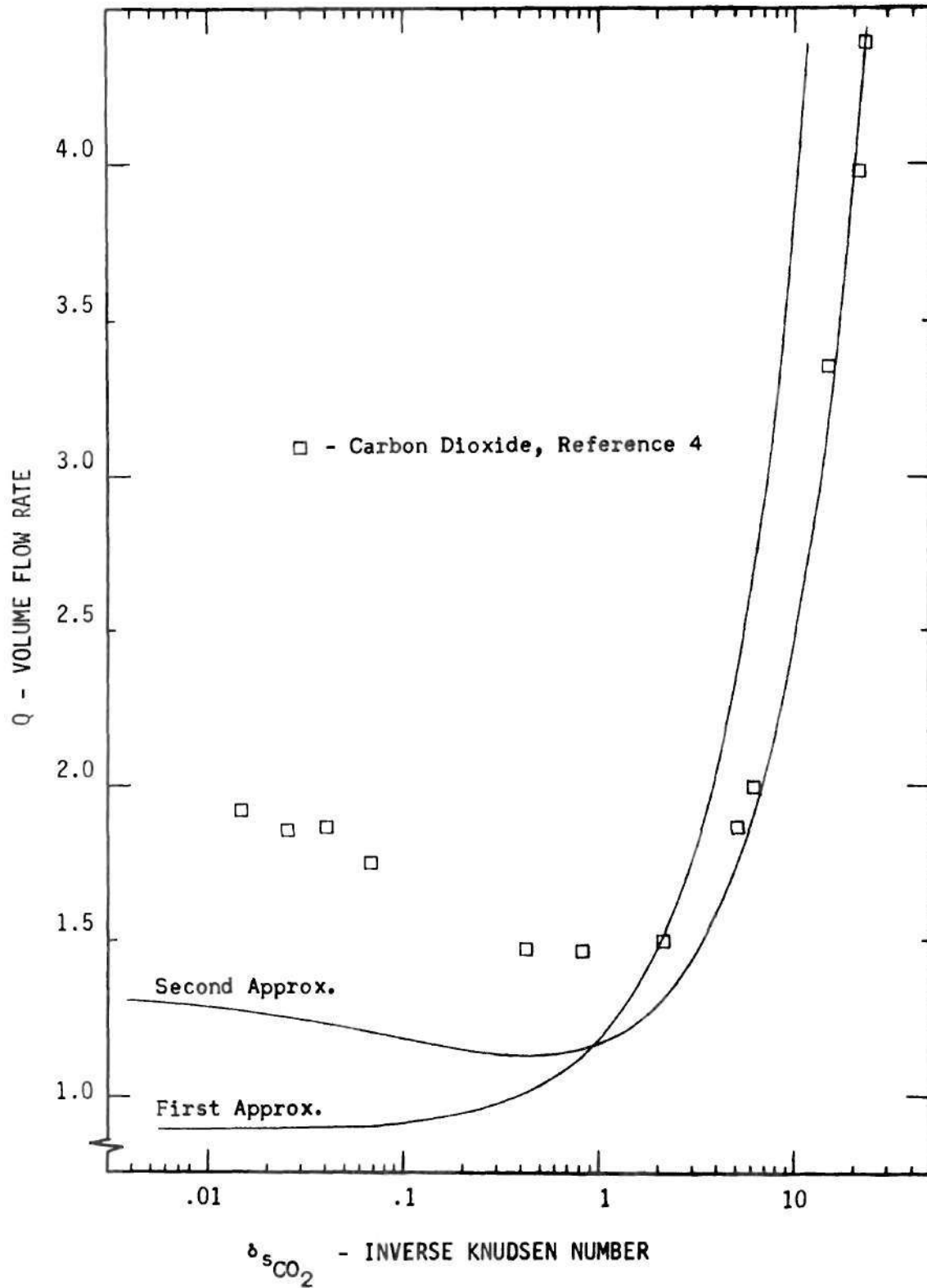


Figure 7. Volume Flow Rate versus Inverse Knudsen Number for the Hard Sphere Model, Carbon Dioxide.

sphere model $I_2/I_3 = 1.086$. Consequently, the half-range character does not disappear away from the walls. In fact, Cercignani points out the half-range character is destroyed only when the molecular model is the Maxwellian one. To correct this observed discrepancy, he proposed the following second-order approximation for the perturbation of the distribution function:

$$h^{*\pm} = a_0^\pm(\eta) c_z + a_1^\pm(\eta) b(\bar{c}) c_x c_z \quad .$$

This form was proposed in order to yield agreement with the Chapman-Enskog solution (34), which is valid away from the walls. Cercignani developed the equations for the solution of the velocity for the Couette flow problem, but did not carry out the calculations because of the complications involved. He also pointed out that the corrections to the half-range solution are probably small.

The objection, although a valid one, does not appear to be an important one. This is because the disappearance of the half-range character should be of importance only in the slip and continuum regions. That is, in these regions, the half-range character must disappear away from the walls because of the large number of molecule-molecule collisions that occur. Therefore, the correction should be of greatest concern for $\delta > 1.0$ approximately. The correction should be of least importance in the near-free-molecular region because, here, the half-range character is preserved throughout the flow field. As seen from a study of the results, the theory closely agrees with the experimental data for the slip and continuum regions. This agreement leads to the conclusion that the half-range moment method as presented in this dissertation does adequately

describe the slip and continuum flow regions for the hard sphere molecules.

Maxwellian Model

First, it is necessary to correct the inverse Knudsen number for the Maxwellian model. For this model, the inverse Knudsen number is given

$$\text{by } \delta_m = 6\sqrt{\pi} A_2(5) \frac{p}{kT} d \sqrt{\frac{R_1}{kT}} \quad . \quad A_2(5) \text{ is a pure number equal to } 0.436,$$

p is the average pressure between the pressure taps for Dong's work, T is the temperature approximately equal to 296°K for all experiments, and R_1 is the force constant for the law of interaction. From Chapman and Cowling (34), page 174, the expression for the coefficient of viscosity for the Maxwellian molecules is

$$\eta = \frac{1}{3\pi} \sqrt{\frac{2m}{R_1}} \frac{kT}{A_2(5)} \quad .$$

From this equation, R_1 can be found for any gas by first knowing the coefficient of viscosity. The following values were found by using the viscosity from reference 32:

$$R_{1\text{H}_2} = 8.456 \times 10^{-44} \text{ dyne} - \text{cm}^5$$

$$R_{1\text{He}} = 3.410 \times 10^{-44} \text{ dyne} - \text{cm}^5$$

$$R_{1\text{CO}_2} = 64.60 \times 10^{-44} \text{ dyne} - \text{cm}^5 \quad .$$

Finally, the inverse Knudsen number for each gas is given by

$$\delta_{mH_2} = 0.0717 p$$

$$\delta_{mHe} = 0.0454 p$$

$$\delta_{mCO_2} = 0.1980 p ,$$

where p is the average pressure measured in microns. From this information it is possible to convert Dong's data to the inverse Knudsen number for Maxwellian molecules.

The results of the first approximation of the volume flow rate are found from equation (96); the results of the second approximation, from equation (98). Tabulated values of $Q(\delta)$ for the second approximation are given in Table 5. The results of the third approximation are obtained from equation (104); the tabulated values are given in Table 6. All of the results are plotted in Figures 8, 9, and 10 for the gases hydrogen, helium, and carbon dioxide, respectively.

Although the second approximation presents a very slight minimum in the transition region, it was felt that the solution was not complete. Thus, a third approximation was calculated, which presents very good results for the transition, slip, and continuum regimes. The minimum is well-placed with respect to the experimental data, although the near-free-molecular results are unsatisfactory. It is expected that higher approximations than the third will yield results that agree better with the data in the free-molecular region. If it were possible to iterate the

Table 5. Volume Flow Rate Versus Inverse Knudsen Number
for the Second Approximation by the Half-Range
Method for the Maxwellian Model

δ	Q	δ	Q
0.01	1.3210	2.60	1.7083
0.05	1.3464	2.70	1.7076
0.10	1.3766	2.80	1.7069
0.20	1.4321	2.90	1.7063
0.30	1.4809	3.00	1.7058
0.40	1.5233	3.10	1.7055
0.50	1.5597	3.20	1.7053
0.60	1.5907	3.30	1.7053
0.70	1.6167	3.40	1.7055
0.80	1.6382	3.50	1.7058
0.90	1.6559	3.60	1.7063
1.00	1.6702	3.70	1.7069
1.10	1.6817	3.80	1.7078
1.20	1.6907	3.90	1.7087
1.30	1.6976	4.00	1.7099
1.40	1.7029	4.50	1.7181
1.50	1.7067	5.00	1.7299
1.60	1.7094	6.00	1.7624
1.70	1.7111	7.00	1.8040
1.80	1.7121	8.00	1.8522
1.90	1.7125	9.00	1.9053
2.00	1.7125	10.00	1.9619
2.10	1.7121	15.00	2.2765
2.20	1.7115	20.00	2.6168
2.30	1.7108	25.00	2.9682
2.40	1.7100	30.00	3.3252
2.50	1.7092	35.00	3.6857

Table 6. Volume Flow Rate Versus Inverse Knudsen Number
for the Third Approximation by the Half-Range
Method for the Maxwellian Model

δ	Q	δ	Q
0.01	1.6090	2.60	1.4947
0.05	1.6487	2.70	1.4927
0.10	1.6890	2.80	1.4913
0.20	1.7421	2.90	1.4903
0.30	1.7659	3.00	1.4898
0.40	1.7692	3.10	1.4897
0.50	1.7595	3.20	1.4899
0.60	1.7422	3.30	1.4906
0.70	1.7210	3.40	1.4915
0.80	1.6984	3.50	1.4928
0.90	1.6758	3.60	1.4943
1.00	1.6541	3.70	1.4962
1.10	1.6337	3.80	1.4982
1.20	1.6151	3.90	1.5005
1.30	1.5981	4.00	1.5030
1.40	1.5827	4.50	1.5184
1.50	1.5690	5.00	1.5375
1.60	1.5567	6.00	1.5838
1.70	1.5459	7.00	1.6373
1.80	1.5363	8.00	1.6955
1.90	1.5280	9.00	1.7570
2.00	1.5207	10.00	1.8209
2.10	1.5143	15.00	2.1598
2.20	1.5089	20.00	2.5140
2.30	1.5043	25.00	2.8744
2.40	1.5004	30.00	3.2379
2.50	1.4972	35.00	3.6030

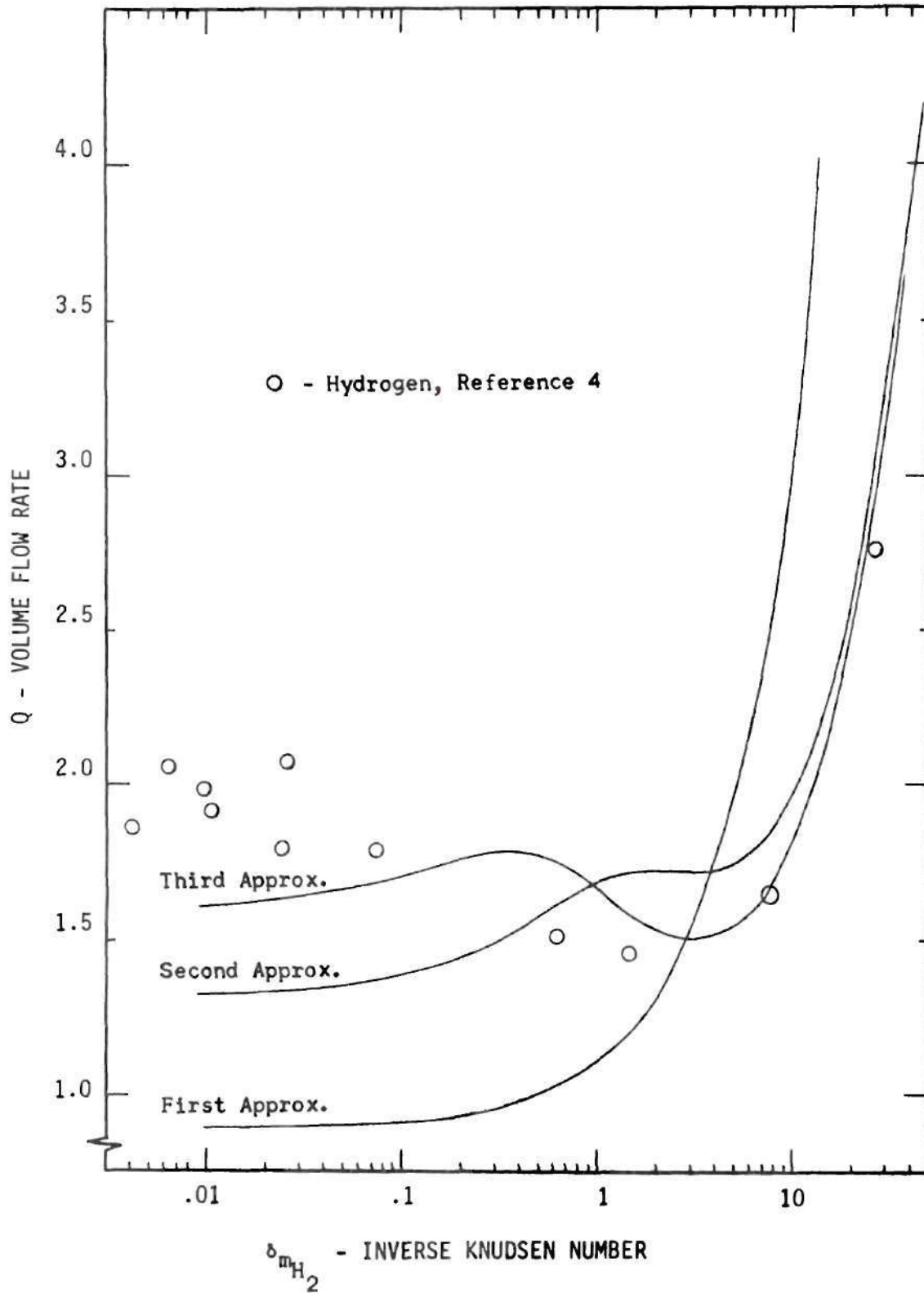


Figure 8. Volume Flow Rate versus Inverse Knudsen Number for the Maxwellian Model, Hydrogen.

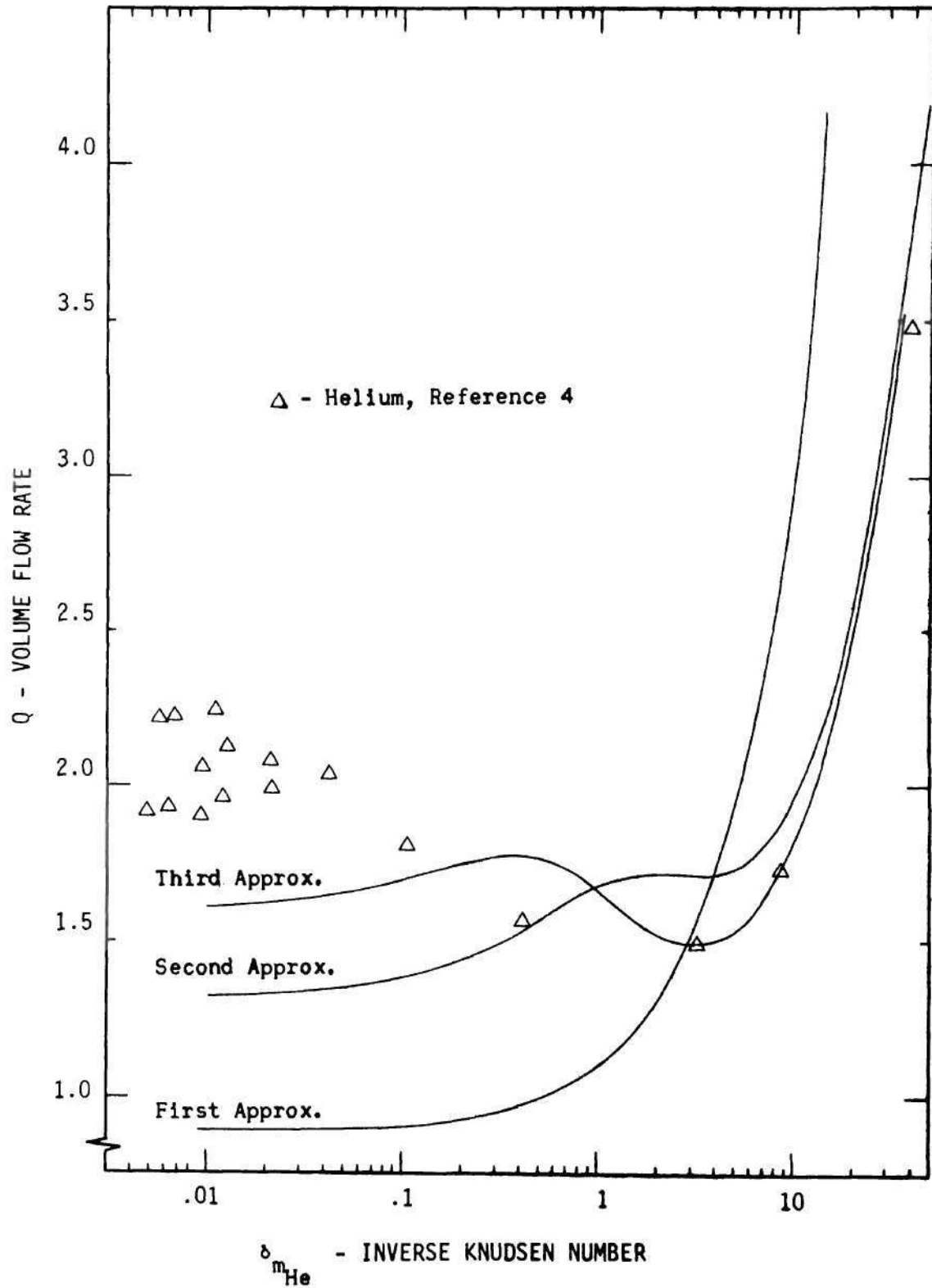


Figure 9. Volume Flow Rate versus Inverse Knudsen Number for the Maxwellian Model, Helium.

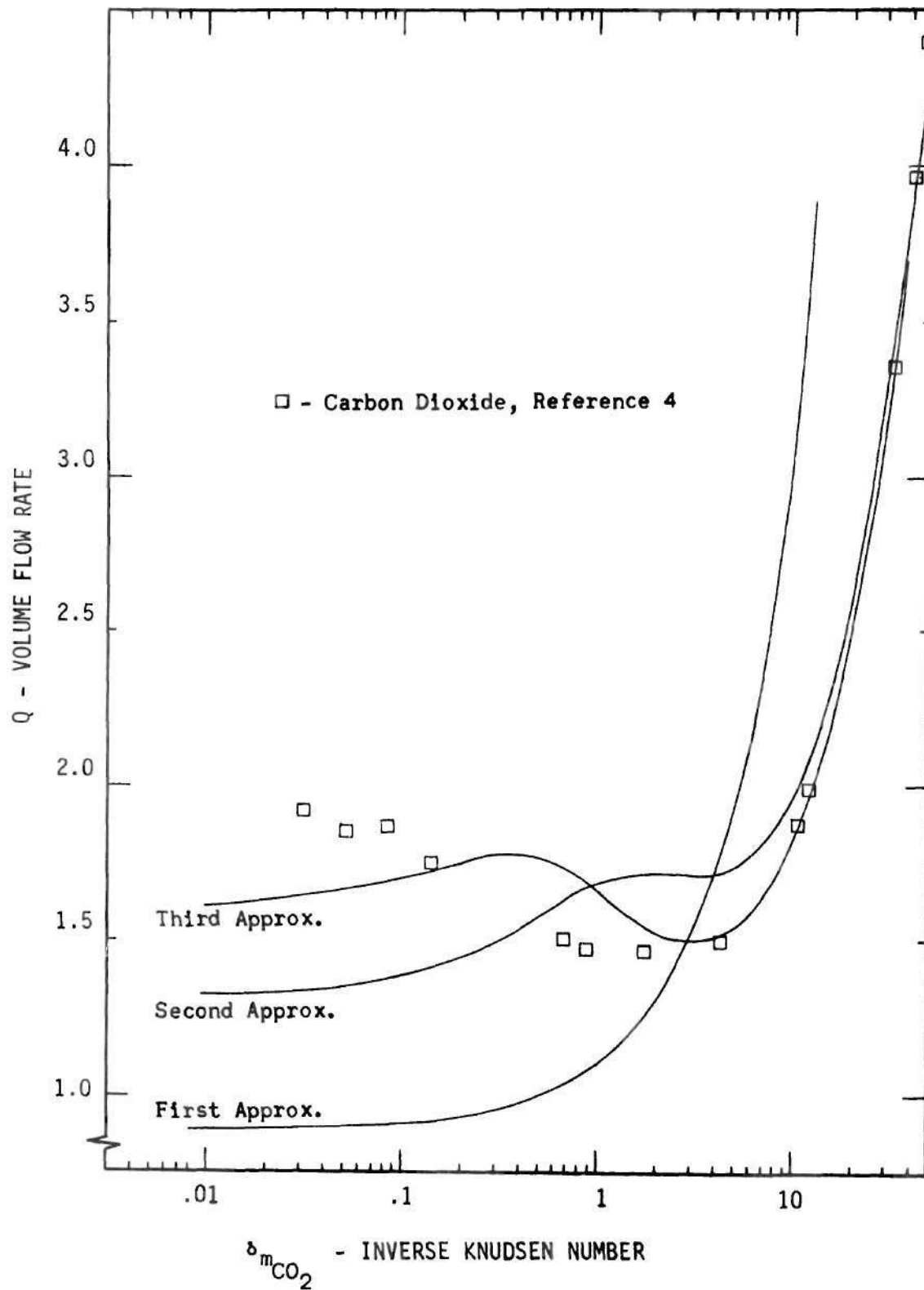


Figure 10. Volume Flow Rate versus Inverse Knudsen Number for the Maxwellian Model, Carbon Dioxide.

solution by the Willis method, the free-molecular limit should more closely follow the data. This idea is based on the results of the investigation of the Krook model by the iteration method.

CHAPTER IV

CONCLUSIONS AND RECOMMENDATIONS

The Boltzmann equation has been analytically solved for the problem of flow between two parallel, infinite plates using the half-range moment method and the Willis iteration method. The study was made for three different molecular models (Krook, hard sphere, and Maxwellian) under the assumption of linear pressure change along the infinite parallel plates. The conclusions are:

1. It is possible to analytically solve the Boltzmann equation for the three different molecular models, obtain a meaningful comparison with the available experimental data, and demonstrate that a minimum exists in the volume flow rate in the transition regime.

2. The full-range method, for the free-molecular to transition regimes, does not yield satisfactory results for the Krook model.

3. The half-range method yields suitable results for the volume flow rate in all flow regimes but the free-molecular. The method gives a minimum in the transition region for the Krook model in the third approximation; for the hard sphere model, in the second approximation; and for the Maxwellian model, in the third approximation.

4. The iteration method of Willis provides very good results for all flow regimes when the first approximation by the half-range method is used as the first guess.

It is recommended that the following be considered for future

investigation:

1. Do not drop the z -dependent terms in the basic integro-differential equation, and solve the problem using boundary conditions at the inlet of the parallel plates.

2. Carry out an extensive experimental program using several different gases and several different parallel-plate geometries. That is, determine the influence of the geometry on the experimental data.

APPENDICES

APPENDIX A

DERIVATION OF EQUATIONS USED IN THE FULL-RANGE
METHOD FOR THE KROOK MODEL

Following the analysis of reference (3), the Boltzmann equation with the Krook model is

$$v_x \frac{\partial f}{\partial x} + v_z \frac{\partial f}{\partial z} = \frac{n}{\sigma_1} (f_{eq} - f) , \quad (A.1)$$

where n/σ_1 is the collision frequency and f_{eq} is the Maxwellian equilibrium distribution function defined as

$$f_{eq} = \frac{n\beta^3}{\pi^{3/2}} e^{-\beta^2(\vec{v} - \vec{u})^2} . \quad (A.2)$$

Following reference (1) and assumptions 1 and 2 on page 11, equation (A.2) becomes

$$f_{eq} = f_0 [1 + 2(\vec{v} \cdot \vec{u})\beta^2] , \quad (A.3)$$

where

$$f_0 = \frac{p_i}{kT} (1 + \kappa z) \frac{\beta^3}{\pi^{3/2}} e^{-\beta^2 \vec{v}^2} , \quad (A.4)$$

and

$$\vec{u} = \frac{1}{\pi^{3/2}} \int \vec{v} f e^{-\vec{v}^2} d^3v .$$

p_i is the inlet pressure, and κ is defined as

$$\kappa = \frac{1}{p_i} \frac{dp}{dz} . \quad (\text{A.5})$$

After approximating the distribution function by a linearized expression, $f = f_0(1 + h)$, and after introducing a dimensionless velocity, $\bar{c} = \beta \bar{v}$, the Boltzmann equation becomes

$$\begin{aligned} c_x \frac{\partial h}{\partial x} + c_z \kappa \left(\frac{1 + h}{1 + \kappa z} \right) + c_z \frac{\partial h}{\partial z} \\ = \beta \frac{n_0}{\sigma_1} [2(\bar{c} \cdot \bar{q}) - h] , \end{aligned} \quad (\text{A.6})$$

where

$$\bar{q} = \frac{1}{\pi^{3/2}} \int \bar{c} h e^{-\bar{c}^2} d^3 c . \quad (\text{A.7})$$

Since it is not possible, at the present, to determine the dependence of h on z , it is assumed that the properties do not vary in the z -direction. Letting $\lambda = \sigma_1 / \beta n_0$, where λ is the mean free path, and noting that the term $(1 + h)$ is of the order of unity, equation (A.6) becomes

$$c_x \frac{dh}{dx} + \kappa c_z + \frac{h}{\lambda} = \frac{2}{\lambda} c_z q_z^* \quad (\text{A.8})$$

where

$$q_z^*(x) = \pi^{-3/2} \int c_z h e^{-\bar{c}^2} d^3 c .$$

Equation (A.8) can be written in a more compact form by defining the inverse Knudsen number $\delta = d/\lambda$, using a nondimensional position coordinate, $\eta = x/d$, and defining $h^* = h/\kappa d$:

$$c_x \frac{dh^*}{d\eta} + c_z + \delta h^* = 2 \delta c_z q_z \quad (\text{A.9})$$

where

$$q_z(\eta) = \pi^{-3/2} \int_{-\infty}^{\infty} c_z h^* e^{-c^2} d^3 c \quad (\text{A.10})$$

The boundary condition for equation (A.9) is developed in equations (16) and (17) of the text.

The volume flow rate is found by first calculating the average velocity at any cross-section,

$$\bar{q}_z^* = \frac{1}{d} \int_{-\frac{d}{2}}^{\frac{d}{2}} q_z^*(x) dx = \kappa d q_{z_{\text{avg}}} \quad .$$

The volume flow rate per unit width of the slit is given by F , such that $F = d \cdot \kappa d q_{z_{\text{avg}}}$. The nondimensional volume flow rate is given by

$$Q = 2 \left[\frac{F}{-d^2 \frac{1}{\rho_i} \frac{dp}{dz}} \right] = 2 \left[\frac{F}{-\kappa d^2} \right]$$

where the factor "2" is used to agree with Cercignani's expression for the volume flow rate. Thus,

$$Q(\delta) = -2q_{z_{\text{avg}}} \quad . \quad (\text{A.11})$$

This is identical to the expression given by Cercignani (3).

In order to develop the moment equations for the full-range method, assume $h^* = c_x \psi$. Equation (A.9) becomes

$$c_x \frac{d\psi}{d\eta} + 1 + \delta\psi = \frac{\delta}{\sqrt{\pi}} \int_{-\infty}^{\infty} \psi e^{-c_x^2} d c_x \quad (\text{A.12})$$

with the boundary condition

$$\psi^{\pm}(\eta = \mp \frac{1}{2}, c_x) = (1 - \alpha)\psi^{\mp}(\eta = \mp \frac{1}{2}, -c_x), \quad (\text{A.13})$$

where the "+" sign indicates $c_x > 0$; the "-" sign, $c_x < 0$. The symmetry condition for the parallel-plate geometry requires that

$$\psi^{\pm}(\eta, c_x) = \psi^{\mp}(-\eta, -c_x).$$

The full-range moments are defined

$$M_k = \int_{-\infty}^{\infty} c_x^k \psi \frac{e^{-c_x^2}}{\sqrt{\pi}} d c_x. \quad (\text{A.14})$$

After multiplying equation (A.12) by $c_x^k \exp(-c_x^2)/\sqrt{\pi}$ and then integrating, the following moment equations are found:

$$\frac{dM_1}{d\eta} = -1$$

$$\frac{dM_2}{d\eta} = -\delta M_1$$

$$\begin{aligned} \frac{dM_{k+1}}{d\eta} + [1 + (-1)^k] \frac{1 \cdot 3 \cdot 5 \cdots (k-1)}{(\sqrt{2})^{k+2}} + \delta M_k \\ = \delta [1 + (-1)^k] \frac{1 \cdot 3 \cdot 5 \cdots (k-1)}{(\sqrt{2})^{k+2}} M_0 \end{aligned} \quad (\text{A.15})$$

Polynomial solutions for ψ are sought, and are expressed in the form

$$\psi(\eta, c_x) = \psi^\pm(\eta, c_x) = \sum_{n=0}^{\infty} c_x^n A_n^\pm(\eta) . \quad (\text{A.16})$$

The half-range character of the A_n^\pm is necessary in order to satisfy the molecular boundary condition. Combining equations (A.14) and (A.15) yields

$$\begin{aligned} M_k = \sum_{n=0}^{\infty} \left\{ A_n^-(\eta) \int_{-\infty}^0 c_x^{n+k} \frac{e^{-c_x^2}}{\sqrt{\pi}} d c_x \right. \\ \left. + A_n^+(\eta) \int_0^{\infty} c_x^{n+k} \frac{e^{-c_x^2}}{\sqrt{\pi}} d c_x \right\} . \end{aligned} \quad (\text{A.17})$$

The boundary condition can now be expressed as

$$A_n^\pm \left(\mp \frac{1}{2} \right) = (1 - \sigma) A_n^\mp \left(\mp \frac{1}{2} \right) . \quad (\text{A.18})$$

Equations (A.15) - (A.18) are used to solve for the velocity which is given by

$$q_z(\eta) = \frac{1}{2\sqrt{\pi}} \int_{-\infty}^{\infty} \psi^\pm e^{-c_x^2} d c_x . \quad (\text{A.19})$$

The volume flow rate is given by equation (A.11).

APPENDIX B

SOLUTION OF THE FIRST APPROXIMATION FOR THE
FULL-RANGE MOMENT METHOD USING
THE KROOK MODEL

Assume $\psi^\pm = A_0^\pm(\eta)$. It is necessary to use the first two unknowns, A_0^+ and A_0^- . The equations are

$$\frac{dM_1}{d\eta} = -1 \quad (\text{B.1})$$

$$\frac{dM_2}{d\eta} = -\delta M_1. \quad (\text{B.2})$$

The solution for M_1 and M_2 is

$$M_1 = -\eta + c_1 \quad (\text{B.3})$$

$$M_2 = \frac{1}{2} \delta \eta^2 - c_1 \delta \eta + c_2. \quad (\text{B.4})$$

According to equation (A.17),

$$M_1 = \frac{1}{2\sqrt{\pi}} (A_0^+ - A_0^-) \quad (\text{B.5})$$

$$M_2 = \frac{1}{4} (A_0^+ + A_0^-) \delta. \quad (\text{B.6})$$

After combining equations (B.3) - (B.6) it is possible to solve for A_0^+ and A_0^- ,

$$A_0^\pm = \delta \eta^2 - (2\delta c_1 \pm \sqrt{\pi})\eta \pm \sqrt{\pi} c_1 + 2c_2. \quad (\text{B.7})$$

The arbitrary constants, c_1 and c_2 , are determined from the boundary conditions,

$$A_0^\pm \left(\mp \frac{1}{2}\right) = (1 - \sigma) A_0^\mp \left(\mp \frac{1}{2}\right). \quad (\text{B.8})$$

The result is

$$\psi^\pm = A_0^\pm = \delta \eta^2 \mp \sqrt{\pi} \eta - \frac{\sqrt{\pi}}{2} \left(\frac{2-\sigma}{\sigma}\right) - \frac{1}{4} \delta \quad (\text{B.9})$$

The velocity is given by equation (A.19) as

$$q_z(\eta) = \frac{1}{2} \delta \eta^2 - \frac{\sqrt{\pi}}{4} \left(\frac{2-\sigma}{\sigma}\right) - \frac{1}{8} \delta. \quad (\text{B.10})$$

Finally, the volume flow rate is found by the use of equation (A.11),

$$Q(\delta) = \frac{1}{6} \delta + \frac{\sqrt{\pi}}{2} \left(\frac{2-\sigma}{\sigma}\right). \quad (\text{B.11})$$

APPENDIX C

DERIVATION OF EQUATIONS USED IN THE HALF-RANGE
METHOD FOR THE KROOK MODEL

The basic integrodifferential equation is (A.9),

$$c_x \frac{dh^{*\pm}}{d\eta} + c_z + \delta h^{*\pm} = 2\pi^{-3/2} \delta c_z \int c_z h^{*\pm} e^{-\bar{c}^2} d^3c. \quad (C.1)$$

Following reference (1), assume $h^{*\pm}$ can be expanded in terms of Hermite polynomials,

$$h^{*\pm} = \sum_{ijk} B_{ijk}^{\pm}(\eta) L_i^{\pm}(c_x) H_j(c_y) H_k(c_z). \quad (C.2)$$

H_j and H_k are the usual Hermite polynomials. $L_i^{\pm}(c_x)$ is an orthogonal polynomial such that

$$\int_0^{\infty} L_i^+ L_l^+ e^{-c_x^2} dc_x = \int_{-\infty}^0 L_i^- L_l^- e^{-c_x^2} dc_x = \sqrt{\pi} \delta_{il}. \quad (C.3)$$

The polynomials are developed by the Gram-Schmidt process and the first few are

$$L_0^{\pm} = \alpha_0$$

$$L_1^{\pm} = \alpha_1 c_x \mp \beta_1$$

$$L_2^{\pm} = \alpha_2 c_x^2 \mp \beta_2 c_x + \gamma_2, \text{ etc.},$$

where

$$\alpha_0 = \sqrt{2}$$

$$\alpha_1 = \sqrt{4\pi/(\pi - 2)}$$

$$\alpha_2 = \sqrt{4(\pi - 2)/(\pi - 3)}$$

$$\beta_1 = \sqrt{4/(\pi - 2)}$$

$$\beta_2 = \sqrt{4\pi/(\pi - 2)(\pi - 3)}$$

$$\gamma_2 = (4 - \pi) / \sqrt{(\pi - 2)(\pi - 3)} .$$

Again following reference (1), multiply equation (C.1) by $L_{\ell}^{\pm}(c_x) H_m(c_y) H_n(c_z) \exp(-c^2)$, use equation (C.2), and integrate over the appropriate half-ranges to obtain

$$\begin{aligned} \frac{d}{d\eta} \left\{ B_{i-1}^{\pm} \frac{\alpha_{i-1}}{\alpha_i} \pm B_i^{\pm} \left(\frac{\beta_{i+1}}{\alpha_{i+1}} - \frac{\beta_i}{\alpha_i} \right) + B_{i+1}^{\pm} \frac{\alpha_i}{\alpha_{i+1}} \right\} \\ + \delta B_i^{\pm} = \left[\frac{\delta}{2} (B_0^+ + B_0^-) - \frac{1}{2\sqrt{2}} \right] \delta_{i0} . \end{aligned} \quad (C.4)$$

The subscripts j and k are dropped since it is a requirement that $j = 0$, $k = 1$, for a non-trivial solution. This requirement means that the expansion of $h^{*\pm}$ takes the form

$$h^{*\pm} = 2c_z \sum_i B_i^{\pm}(\eta) L_i^{\pm}(c_x)$$

which is a polynomial in c_x , similar to the full-range expansion.

The expression for $q_z(\eta)$ is found by substituting equation (C.2) into equation (A.10). The result is

$$q_z(\eta) = \pi^{-3/2} \sum_{ijk} B_{ijk}^{\pm} \int_{-\infty}^{\infty} L_i^{\pm}(c_x) e^{-c_x^2} d c_x \cdot \int_{-\infty}^{\infty} H_j(c_y) e^{-c_y^2} d c_y \int_{-\infty}^{\infty} c_z H_k(c_z) e^{-c_z^2} d c_z . \quad (C.5)$$

It can be shown by computing the last two integrals that if $j \neq 0$, $k \neq 1$, then $q_z(\eta) = 0$. Thus, for $j = 0$, $k = 1$,

$$q_z(\eta) = \frac{1}{\sqrt{\pi}} \sum_i \left[B_i^- \int_{-\infty}^0 L_i^- e^{-c_x^2} d c_x + B_i^+ \int_0^{\infty} L_i^+ e^{-c_x^2} d c_x \right]. \quad (C.6)$$

By carrying out the integration in equation (C.6), it is possible to demonstrate that the velocity is given by

$$q_z(\eta) = \frac{1}{\sqrt{2}} (B_0^+ + B_0^-) . \quad (C.7)$$

As in the full-range method, $Q(\delta) = -2q_{z_{avg}}$.

The symmetry condition for the physical problem is

$$h^{*\pm}(\eta, c_x) = h^{*\mp}(-\eta, -c_x) ,$$

which reduces to

$$B_i^{\pm}(\eta) = (-1)^i B_i^{\mp}(-\eta) . \quad (C.8)$$

The boundary condition is similar to that of the full-range method,

$$h^{*\pm}(\eta = \mp \frac{1}{2}, c_x) = (1 - \sigma)h^{*\mp}(\eta = \mp \frac{1}{2}, -c_x). \quad (\text{C.9})$$

This reduces to

$$B_i^{\pm}(\mp \frac{1}{2}) = (1 - \sigma)(-1)^i B_i^{\mp}(\mp \frac{1}{2}). \quad (\text{C.10})$$

APPENDIX D

SOLUTION OF THE SECOND APPROXIMATION FOR THE
 HALF-RANGE MOMENT METHOD USING
 THE KROOK MODEL

From Appendix C, equation (C.4), four equations are obtained when all $B_i^\pm = 0$, $i \geq 2$:

$$\frac{dB_0^\pm}{d\eta} \pm \sqrt{\frac{\pi-2}{2}} \frac{dB_1^\pm}{d\eta} \mp \frac{\sqrt{\pi}}{2} \delta (B_0^+ - B_0^-) = \mp \frac{\sqrt{\pi}}{2\sqrt{2}} \quad (D.1)$$

$$\frac{dB_0^\pm}{d\eta} \pm \frac{2\sqrt{2}}{(\pi-2)^{3/2}} \frac{dB_1^\pm}{d\eta} + \sqrt{\frac{2\pi}{\pi-2}} \delta B_1^\pm = 0. \quad (D.2)$$

The particular solution is obtained by assuming B_0^\pm and B_1^\pm are polynomials in η . In general, it is not necessary to assume that terms higher than the second order are present. For example, if it were assumed that B_0^+ were given by a tenth-order polynomial, it would be found that the coefficients of η^3 , η^4 , etc., were all zero. By following this procedure, it is assumed that

$$B_0^\pm = b_0 \pm b_1\eta + b_2\eta^2 \quad (D.3)$$

$$B_1^\pm = \pm b_3 + b_4\eta, \quad (D.4)$$

where the symmetry condition is used to find B_0^- and B_1^- . After

substituting equations (D.3) and (D.4) into equations (D.1) and (D.2), the particular solution is found to be

$$b_1 = -1/\sqrt{2\pi} \quad (D.5)$$

$$b_2 = \sqrt{2} \delta / 4 \quad (D.6)$$

$$b_3 = 1/(2\delta \sqrt{\pi-2}) \quad (D.7)$$

$$b_4 = -\sqrt{(\pi-2)/4\pi} . \quad (D.8)$$

b_0 must be determined by one of the boundary conditions after the complete solution is found.

The homogeneous set of equations is obtained from (D.1) and (D.2) by setting the right-hand side of equation (D.1) equal to zero. The solution is assumed to be

$$B_i^\pm = \sum_j g_{ij}^\pm e^{aj\delta\eta} . \quad (D.9)$$

Substituting equation (D.9) into the homogeneous set yields

$$\alpha g_0^\pm \pm \sqrt{\frac{\pi-2}{2}} \alpha g_1^\pm \pm \frac{\sqrt{\pi}}{2} (g_0^+ - g_0^-) = 0 \quad (D.10)$$

$$\alpha g_0^\pm \pm \frac{2\sqrt{2}}{(\pi-2)^{3/2}} \alpha g_1^\pm + \sqrt{\frac{2\pi}{\pi-2}} g_1^\pm = 0 . \quad (D.11)$$

If a solution of the above set of equations exists, then the determinant of the coefficient matrix must be zero. This condition yields the values of α :

$$\alpha = \pm \sqrt{2} \left(\frac{\pi - 2}{4 - \pi} \right) . \quad (D.12)$$

It is now possible to solve for three of the four unknowns in terms of the remaining unknown. Let $g_0^- = \ell g_0^+$, $g_1^+ = m g_0^+$, and $g_1^- = n g_0^+$. Any three of the equations (D.10) and (D.11) can be used to solve for ℓ , m , and n . The results are $\ell = 2.6726$, $m = -0.2804$, and $n = 2.4943$. Finally, the complete solution for the unknowns is expressed as the sum of the particular solution and the homogeneous solution,

$$B_0^\pm = b_0 \pm b_1 \eta + b_2 \eta^2 + g_0^\pm e^{\pm \alpha \delta \eta} + \ell g_0^\pm e^{\mp \alpha \delta \eta} \quad (D.13)$$

$$B_1^\pm = \pm b_3 + b_4 \eta \pm m g_0^\pm e^{\pm \alpha \delta \eta} \mp \eta g_0^\pm e^{\mp \alpha \delta \eta} . \quad (D.14)$$

The boundary condition, equation (C.9), is used to determine the two unknowns b_0 and g_0^+ . They are

$$g_0^+ = \frac{\frac{b_4}{2} - b_3}{m e^{-\alpha \delta / 2} - n e^{\alpha \delta / 2}} \quad (D.15)$$

$$b_0 = \frac{b_1}{2} - \frac{b_2}{4} - g_0^+ (e^{-\alpha \delta / 2} + \ell e^{\alpha \delta / 2}) . \quad (D.16)$$

The velocity is determined by equation (C.6),

$$q_z(\eta) = \frac{1}{\sqrt{2}} (B_0^+ + B_0^-) .$$

The volume flow rate is $Q(\delta) = -2q_{z,avg}$.

APPENDIX E

DERIVATION OF THE FREE-MOLECULAR LIMIT FOR
THE VOLUME FLOW RATE USING THE WILLIS
ITERATION METHOD

A property of the solutions by the half-range moment method is that

$$\lim_{\delta \rightarrow 0} q_z(\eta) = \text{const.},$$

where the constant is different for each approximation. Using this property, it is possible to examine the Willis iteration procedure in the limit as $\delta \rightarrow 0$. Thus, assume $q_z(\eta^i) = \text{const.} = c_1$ for a first guess. After substitution of this first guess into equation (54) of the text, the first iteration for $q_z(\eta^i)$ can be written

$$q_z(\eta) = \frac{1}{2\sqrt{\pi}} \left[\int_0^{\infty} e^{-c^2 x} (4c_1 - 2/\delta) dc_x \right. \\ \left. + \int_0^{\infty} e^{-c^2 x} (-2c_1 + 1/\delta) (e^{-(\eta + \frac{\pi}{2})\delta/c_x} + e^{-(\frac{1}{2} - \eta)\delta/c_x}) dc_x \right]. \quad (\text{E.1})$$

After carrying out the integration, the result is

$$q_z(\eta) = c_1 - \frac{1}{2\delta} + \left(\frac{1}{2\sqrt{\pi}\delta} - \frac{c_1}{\sqrt{\pi}} \right) [f_0(x_1) + f_0(x_2)], \quad (\text{E.2})$$

where

$$f_0(x) = \int_0^{\infty} e^{-u^2 - x/u} du$$

$$x_1 = \left(\eta + \frac{1}{2}\right) \delta$$

$$x_2 = \left(\frac{1}{2} - \eta\right) \delta .$$

To examine $q_z(\eta)$ as $\delta \rightarrow 0$, it is necessary to study the limit of $f_0(x)$ for small x . Abramowitz gives the limit

$$\lim_{x \rightarrow 0} f_0(x) = \frac{\sqrt{\pi}}{2} + x \ln x$$

Using this limit in equation (E.2), the velocity becomes

$$q_z(\eta) = \left(\frac{1}{2\sqrt{\pi}\delta} - \frac{c_1}{\sqrt{\pi}}\right) \left[\delta\left(\eta + \frac{1}{2}\right) \ln\left(\eta + \frac{1}{2}\right) + \delta\left(\frac{1}{2} - \eta\right) \ln\left(\frac{1}{2} - \eta\right) + \delta \ln \delta\right]. \quad (\text{E.4})$$

The average velocity at any cross-section is obtained by integrating $q_z(\eta)$ from $\eta = -1/2$ to $\eta = +1/2$. Then, the volume flow rate is given by $Q(\delta) = -2q_{z_{\text{avg}}}$. Thus,

$$Q(\delta \rightarrow 0) = \frac{1}{2\sqrt{\pi}} - \frac{1}{\sqrt{\pi}} \ln \delta + c_1 \left[\frac{\delta}{\sqrt{\pi}} (2 \ln \delta - 1)\right]. \quad (\text{E.5})$$

The limit of the term in the square brackets is zero as $\delta \rightarrow 0$. Thus, $Q(\delta \rightarrow 0)$ is independent of the first guess used in the iteration scheme. The volume flow rate is

$$Q(\delta \rightarrow 0) = \frac{1}{2\sqrt{\pi}} - \frac{1}{\sqrt{\pi}} \ln \delta . \quad (\text{E.6})$$

For very small δ ,

$$Q(\delta \rightarrow 0) = - \frac{1}{\sqrt{\pi}} \ln \delta ,$$

which agrees with the asymptotic expression derived by Cercignani (3).

APPENDIX F

SOLUTION OF THE SECOND APPROXIMATION FOR THE
HALF-RANGE MOMENT METHOD USING THE
HARD SPHERE MODEL

The basic equation is (59) in the text,

$$c_x \frac{dh^{*\pm}}{d\eta} + c_z = \delta_s J(h^{*\pm}), \quad (\text{F.1})$$

where $J(h^{*\pm})$ is defined by equation (61) of the text and the inverse Knudsen number is $\delta_s = dn_0 \sqrt{2} \pi a^2$. For the second approximation, assume

$$h^{*\pm} = a_0^\pm c_z + a_1^\pm c_z c_x. \quad (\text{F.2})$$

Following reference (19)

$$\begin{aligned} J(h^{*\pm}) = & \frac{a_0^+ + a_0^-}{2} J(c_z) + \frac{a_1^+ + a_1^-}{2} J(c_z c_x) \\ & + \frac{a_0^+ - a_0^-}{2} J(c_z \text{ sign } c_x) + \frac{a_1^+ - a_1^-}{2} J(c_z c_x \text{ sign } c_x). \end{aligned} \quad (\text{F.3})$$

After multiplying equation (F.1) by $c_z (1 \pm \text{sign } c_x) e^{-\frac{c^2}{2}}$, using equations (F.2) and (F.3), and integrating, the following equation is obtained:

$$\frac{da_0^\pm}{d\eta} \pm \frac{\sqrt{\pi}}{2} \frac{da_1^\mp}{d\eta} \pm \sqrt{\pi} = \frac{1}{\pi} [I_2(a_1^+ + a_1^-) + I_1(a_0^+ - a_0^-)]. \quad (\text{F.4})$$

After multiplying equation (F.1) by $c_z c_x (1 \pm \text{sign } c_x) e^{-c^2}$ and following the same procedure as above, the second equation is

$$\begin{aligned} \frac{da_0^\pm}{d\eta} \pm \frac{2}{\sqrt{\pi}} \frac{da_1^\pm}{d\eta} \pm \frac{2}{\sqrt{\pi}} &= \frac{2}{\pi \sqrt{\pi}} [I_3(a_1^+ + a_1^-) \\ &+ I_2(a_0^+ - a_0^-) \pm I_4(a_1^+ - a_1^-)] , \end{aligned} \quad (\text{F.5})$$

where I_1 , I_2 , I_3 , and I_4 are the bracket integrals discussed in the text. Their values are

$$I_1 = -1.0059 \pi$$

$$I_2 = -0.4345 \pi$$

$$I_3 = -0.4000 \pi$$

$$I_4 = -1.6982 \pi .$$

Equations (F.4) and (F.5) are solved for a_0^\pm and a_1^\pm in a manner similar to that presented in Appendix D for the Krook model.

The particular solution is assumed to be

$$a_0^\pm = b_0 \pm b_1 \eta + b_2 \eta^2 \quad (\text{F.6})$$

$$a_1^\pm = \pm b_3 + b_4 \eta . \quad (\text{F.7})$$

After substituting equations (F.6) and (F.7) into equations (F.5) and (F.4), the particular solution is found to be

$$b_1 = -0.06304$$

$$b_2 = + 0.9015 \delta_s$$

$$b_3 = + 0.2899/\delta_s$$

$$b_4 = -1.9289$$

b_0 is determined by one of the boundary conditions after the complete solution is found.

The homogeneous set of equations is obtained from equations (F.4) and (F.5) by dropping the terms $\pm \sqrt{\pi}$ and $\pm 2/\sqrt{\pi}$, respectively. The solution is assumed to be of the form

$$a_i^\pm = \sum_j g_{ij}^\pm e^{a_j b_s \eta} \quad (F.8)$$

Substituting equation (F.8) into the homogeneous set yields

$$\alpha g_0^\pm \pm \frac{\sqrt{\pi}}{2} \alpha g_1^\pm - \frac{I_2}{\pi} (g_1^+ + g_1^-) - \frac{I_1}{\pi} (g_0^+ - g_0^-) = 0 \quad (F.9)$$

$$\alpha g_0^\pm \pm \frac{2}{\sqrt{\pi}} \alpha g_1^\pm - \frac{2}{\pi \sqrt{\pi}} I_3 (g_1^+ + g_1^-) - \frac{2}{\pi \sqrt{\pi}} I_2 (g_0^+ - g_0^-)$$

$$\mp \frac{2}{\pi \sqrt{\pi}} I_4 (g_1^+ - g_1^-) = 0 \quad (F.10)$$

Setting the determinant of the coefficient matrix equal to zero yields $\alpha = \pm 7.8698$. Following Appendix D, $l = -4.3806$, $m = -1.5262$, and $n = -4.5452$.

The complete solution for the unknowns is

$$a_0^\pm = b_0 \pm b_1 \eta + b_2 \eta^2 + g_0^+ (e^{\pm \alpha \delta_s \eta} + l e^{\mp \alpha \delta_s \eta}) \quad (\text{F.11})$$

$$a_1^\pm = \pm b_3 + b_4 \eta \pm g_0^+ (m e^{\pm \alpha \delta_s \eta} - n e^{\mp \alpha \delta_s \eta}) . \quad (\text{F.12})$$

b_0 and g_0^+ are found from the boundary conditions;

$$a_0^+(-\frac{1}{2}) = (1 - \sigma) a_0^-(-\frac{1}{2}), \quad a_1^+(-\frac{1}{2}) = (1 - \sigma) a_1^-(-\frac{1}{2}) . \quad (\text{F.13})$$

The equations for b_0 and g_0^+ are presented in the text, equations (83) and (84). The velocity is given by

$$q_z(\eta) = \frac{1}{4} \left[a_0^+ + a_0^- + \frac{a_1^+ - a_1^-}{\sqrt{\pi}} \right] . \quad (\text{F.14})$$

The expressions for $q_z(\eta)$ and $Q(\delta_s)$ are presented in equations (82) and (85) of the text.

APPENDIX G

THE CALCULATION OF I_8 FOR THE MAXWELLIAN MODEL

Since the calculation of I_8 is quite long, only the major points of the solution are presented. The calculation of I_9 is similar, but much longer.

The bracket integral I_8 is defined $I_8 = [c_z c_x^2 \text{sign } c_x, c_z \text{sign } c_x]$. Following equation (67) of the text, I_8 is written

$$I_8 = \frac{1}{6\pi^2 A_2(5)} \sqrt{\frac{m}{2R_1}} \int e^{-(c_1^2 + c^2)} d^3 c_1 d^3 c \int \sin \theta F(\theta, R_1) d\theta dc$$

$$\cdot c_z c_x^2 \text{sign } c_x \left[c_{z_1}' \text{sign } c_{x_1}' + c_z' \text{sign } c_x' - c_{z_1} \text{sign } c_{x_1} - c_z \text{sign } c_x \right], \quad (G.1)$$

where $A_2(5) = 0.436$, $F(\theta, R_1)$ is defined

$$F(\theta, R_1) = \sqrt{\frac{m}{2R_1}} v_r I(v_r, \theta), \quad (G.2)$$

and

$$\text{sign } c_x = -\frac{i}{\pi} \int_{-\infty}^{\infty} e^{itc_x} \frac{dt}{t}. \quad (G.3)$$

In order to simplify the integration of equation (G.1), divide the integration into four parts such that $I_8 = I_{8a} + I_{8b} + I_{8c} + I_{8d}$,

where I_{θ_a} is the integration over c'_{z_1} sign c'_{x_1} , etc. The following relations can be obtained from a study of the equations for c'_{x_1} , c'_{z_1} , c'_{z_1} :

$$\begin{aligned} I_{\theta_b}(\theta) &= I_{\theta_a}(\theta + \pi) \\ I_{\theta_c}(\theta) &= I_{\theta_a}(\theta = 0) \\ I_{\theta_d}(\theta) &= I_{\theta_a}(\theta = \pi) \end{aligned} \quad (G.4)$$

Thus, it is necessary to calculate only I_{θ_a} . I_{θ_a} is equal to

$$\begin{aligned} I_{\theta_a} &= \frac{1}{6\pi^2 A_2(5)} \sqrt{\frac{m}{2R_1}} \left[-\frac{1}{\pi^2} \int_{-\infty}^{\infty} \frac{dt}{t} \int_{-\infty}^{\infty} \frac{ds}{s} \int_0^{\infty} \exp(-2v_c^2) v_c dv_c \right. \\ &\quad \cdot \int_0^{\infty} \exp(-v_r^2/2) v_r dv_r \int_{-\infty}^{\infty} dv_{c_x} \exp(-2v_{c_x}^2) \int_{-\infty}^{\infty} \exp(-v_{r_x}^2/2) dv_{r_x} \\ &\quad \cdot \int_0^{2\pi} d\theta_c \int_0^{2\pi} d\theta_r \int_0^{2\pi} d\epsilon \int_0^{\pi} \sin \theta F(\theta, R_1) d\theta c_z^2 c_x^2 c_{z_1}' \\ &\quad \left. \cdot \exp(itc_x) \exp(itc_{x_1}') \right]. \quad (G.5) \end{aligned}$$

c'_{x_1} and c'_{z_1} are defined in equations (70) and (71) of the text. Polar coordinates are used for v_c and v_r such that

$$\begin{aligned} v_r^2 &= v_{r_x}^2 + v_{r_y}^2 + v_{r_z}^2 & v_c^2 &= v_{c_x}^2 + v_{c_y}^2 + v_{c_z}^2 \\ v_{r_x} &= v_{r_x} & v_{c_x} &= v_{c_x} \end{aligned}$$

$$\begin{aligned} v_{r_y} &= v_r \cos \theta_r & v_{c_y} &= v_c \cos \theta_c \\ v_{r_z} &= v_r \sin \theta_r & v_{c_z} &= v_c \sin \theta_c \end{aligned}$$

The integrations are most easily carried out in the following order: θ_c , θ_r , v_c , ε , v_r , v_{c_x} , v_{r_x} , s , t , and the final numerical integration over θ . After integration over θ_c and θ_r , I_{8_a} is equal to

$$\begin{aligned} I_{8_a} &= \frac{-2}{6\pi^2 A_2(5)} \sqrt{\frac{m}{2R_1}} \left[\int_{-\infty}^{\infty} \frac{dt}{t} \int_{-\infty}^{\infty} \frac{ds}{s} \int_0^{\infty} \exp(-2v_c^2) v_c dv_c \right. \\ &\quad \cdot \int_0^{\infty} \exp(-v_r^2/2) v_r dv_r \int_{-\infty}^{\infty} \exp(-2v_{c_x}^2) dv_{c_x} \int_{-\infty}^{\infty} \exp(-v_{r_x}^2/2) dv_{r_x} \\ &\quad \cdot \int_0^{2\pi} d\varepsilon \int_0^{\pi} \sin \theta F(\theta, R_1) d\theta \left(v_c^2 - \frac{1}{4} v_r^2 \cos^2 \theta - \frac{1}{4} v_r v_{r_x} \sin \theta \cos \varepsilon \right) \\ &\quad \cdot \left(v_{c_x} + v_{r_x} \right)^2 \exp[i(s+t)v_{c_x}] \exp\left[-\frac{i}{2}(t-s \cos \theta)v_{r_x}\right] \\ &\quad \left. \cdot \exp\left[-\frac{i}{2}s v_r \sin \theta \cos \varepsilon\right] \right] \quad (G.6) \end{aligned}$$

The integrals over s and t are found in reference 37. The results after integration over all variables except θ is

$$I_{8_a} = \frac{-1}{6\pi^2 A_2(5)} \sqrt{\frac{m}{2R_1}} \left[\pi^3 \int_0^{\pi} \sin \theta F(\theta, R_1) G_a(\theta) d\theta \right] \quad (G.7)$$

where

$$\begin{aligned}
G_a(\theta) = & -b(\sin^{-1} b) + \frac{2}{(1-b^2)^{1/2}} \left[-\frac{1}{4} ab^2 - \frac{1}{8} ab + b^2 \right. \\
& \left. + \frac{7}{16} a - b \right] + \frac{4}{(1-b^2)^{3/2}} \left[\frac{1}{128} a^2 - \frac{1}{32} a - \frac{1}{32} ab \right. \\
& \left. + \frac{1}{16} ab^2 \right] \quad (G.8)
\end{aligned}$$

and

$$a = \sin^2 \theta, \quad b = \sin^2 \frac{\theta}{2}.$$

I_8 is now written

$$I_8 = \frac{1}{6\pi^2 A_2(5)} \sqrt{\frac{m}{2R_1}} \left[-\pi^3 \int_0^\pi \sin \theta F(\theta, R_1) G(\theta) d\theta \right], \quad (G.9)$$

where $G(\theta) = G_a(\theta) + G_a(\theta + \pi) - G_a(0) - G_a(\pi)$. In order to determine $G_a(\pi)$, go back to the integration over s and t , set $\theta = \pi$ and then carry out the integration.

The remainder of the calculation is straightforward and is illustrated by equations (89) - (94) of the text. The procedure is the same for each bracket integral which must be calculated numerically.

LITERATURE CITED

1. E. P. Gross, E. A. Jackson, and S. Ziering, "Boundary Value Problems in Kinetic Theory of Gases," Annals of Physics 1, 141 (1957).
2. D. R. Willis, A Study of some Nearly Free Molecular Flow Problems, Princeton University, Ph. D. Thesis, 1958.
3. C. Cercignani and A. Daneri, "Flow of a Rarefied Gas between Two Parallel Plates," Journal of Applied Physics 34, 3509 (1963).
4. W. Dong, Vacuum Flow of Gases through Channels with Circular, Annular, and Rectangular Cross Sections, University of California, Ph. D. Thesis, 1956.
5. M. Knudsen, "Die Gesetze der Molekularströmung und der inneren Reibungsströmung der Gase durch Röhren," Annalen der Physik 28, series 4, 75 (1909).
6. M. Knudsen, "Molekularströmung des Wasserstoffs durch Röhren und das Hitzdrahtmanometer," Ann. Phys. 35, series 4, 389 (1911).
7. M. Knudsen, Kinetic Theory of Gases, Third Ed., John Wiley and Sons, Inc., New York, 1950.
8. M. V. Smoluchowski, "Zur kinetischen Theorie der Transpiration und Diffusion verdünnter Gase," Ann. Phys. 33, series 4, 1559 (1910).
9. W. Gaede, "Die äussere Reibung der Gase," Ann Phys. 41, series 4, 289 (1913).
10. P. Clausing, "Über die Strömung sehr verdünnter Gase durch Röhren von beliebiger Länge," Ann. Phys. 12, series 5, 961 (1932).
11. R. E. H. Rasmussen, "Über die Strömung von Gasen in engen Kanälen," Ann. Phys. 29, series 5, 665 (1937).
12. J. W. Hiby and M. Pahl, "Der Einfluss von Zweierstössen auf die molekulare Gasströmung," Zeitschrift für Naturforschung 7a, 542 (1952).
13. W. G. Pollard and R. D. Present, "On Gaseous Self-Diffusion in Long Capillary Tubes," Physical Review 73, 762 (1948).
14. K. Takao, "Rarefied Gas Flow between Two Parallel Plates," in Rarefied Gas Dynamics (ed. L. Talbot), Academic Press, Inc., New York, 465 (1961).

15. S. Ziering, "Plane Poiseuille Flow," in Rarefied Gas Dynamics (ed. L. Talbot), Academic Press, Inc., New York, 451 (1961).
16. C. Cercignani, "Plane Poiseuille Flow and Knudsen Minimum Effect," in Rarefied Gas Dynamics (ed. Laurmann), Academic Press, Inc., New York, 92 (1963).
17. V. Kourganoff and I. W. Busbridge, Basic Methods in Transfer Problems, Oxford University Press, London, 1952.
18. E. P. Gross and S. Ziering, "Theory of Transfer Processes," Astrophysical Journal 123, 343 (1956).
19. E. P. Gross and S. Ziering, "Kinetic Theory of Linear Shear Flow," Physics of Fluids 1, 215 (1958).
20. E. P. Gross and S. Ziering, "Heat Flow between Parallel Plates," Phys. of Fluids 2, 701 (1959).
21. S. Ziering, "Shear and Heat Flow for Maxwellian Molecules," Phys. of Fluids 3, 503 (1960).
22. P. L. Bhatnager, E. P. Gross, and M. Krook, "A Model for Collision Processes in Gases," Phys. Rev. 94, 511 (1954).
23. M. Abramowitz, "Evaluation of the Integral $\int_0^{\infty} \exp(-u^2 - x/u) du$," Journal of Mathematics and Physics 32, 188 (1953).
24. D. R. Willis, "Linearized Couette Flow for Arbitrary Knudsen Numbers," Kth Aero TN 52, Royal Institute of Technology, (1960).
25. S. Ziering, On Transport Theory of Rarefied Gases, Syracuse University, Ph. D. Thesis, 1958.
26. J. Jeans, The Dynamical Theory of Gases, Dover Publications, Inc., New York, 1954.
27. R. D. Present, Kinetic Theory of Gases, McGraw-Hill Book Company, New York, 1958.
28. Wang Chang and Uhlenbeck, "Propagation of Sound in Monatomic Gases," Engineering Research Institute, University of Michigan, (1952).
29. H. J. M. Hanley and W. A. Steele, "Low Pressure Flow of Gases," Journal of Physical Chemistry 68, 3087 (1964).
30. E. P. Gross and E. A. Jackson, "Kinetic Models and the Linearized Boltzmann Equation," Phys. of Fluids 2, 432 (1959).

31. M. Abramowitz and I. A. Stegun (editors), Handbook of Mathematical Functions, National Bureau of Standards Applied Mathematics Series 55, 1964.
32. G. D. Hodgman (ed.), Handbook of Chemistry and Physics, Thirty-Sixth Edition, Chemical Rubber Publishing Co., 1955.
33. C. Cercignani, "Shear Flow for Gas Molecules Interacting with an Arbitrary Central Force," Il Nuovo Cimento 27, 1240 (1963).
34. S. Chapman and T. G. Cowling, The Mathematical Theory of Non-Uniform Gases, Cambridge University Press, 1964.
35. A. B. Huang and D. P. Giddens, "The Discrete Ordinate Method for the Linearized Boundary Value Problems in the Kinetic Theory of Gases," To be presented at the Fifth International Symposium on Rarefied Gas Dynamics at Oxford University, Oxford, England, July 4-8, 1966.
36. J. C. Maxwell, "The Dynamical Theory of Gases," in The Scientific Papers of James Clerk Maxwell (ed. W. D. Niven), vol. II, Dover Publications, Inc., New York, 1952.
37. Wang Chang and Uhlenbeck, "Transport Phenomena in Very Dilute Gases," Engineering Research Institute, University of Michigan, Report No. CM 579, 1949.
38. J. O. Hirshfelder, C. F. Curtiss and R. B. Bird, Molecular Theory of Gases and Liquids, John Wiley and Sons, Inc., New York, p. 545, 1964.

VITA

Robert Lee Stoy, Jr., was born in Washington, D. C., on January 4, 1942. He attended elementary and high schools in McLean, Virginia, and was graduated from McLean High School in 1959.

He entered the Georgia Institute of Technology in September of 1959, as a student on the co-operative plan. His employer at this time was General Dynamics - Fort Worth. In December, 1961, he continued school as a regular student. In September of 1963, he received the degree of Bachelor of Aerospace Engineering (with highest honor).

He continued his studies at the Georgia Institute of Technology as a graduate student, receiving a three-year NASA Fellowship. He received the degree of Master of Science in Aerospace Engineering in June, 1965. He is a member of Tau Beta Pi, Sigma Gamma Tau, Phi Kappa Phi, and Sigma Xi.

In December of 1964, he married the former Sara Louise Gilbertson of Arlington, Virginia.